RSC Advances

PAPER

View Article Online
View Journal | View Issue

Cite this: *RSC Adv.*, 2021, **11**, 2487

The design, synthesis, and *in vitro* trypanocidal and leishmanicidal activities of 1,3-thiazole and 4-thiazolidinone ester derivatives

Muhammad Haroon,[a] Mabilly Cox Holanda de Barros Dias,[b] Aline Caroline da Silva Santos,[c] Valéria Rêgo Alves Pereira,[c] Luiz Alberto Barros Freitas,[b] Rodolfo Bento Balbinot,[d] Vanessa Kaplum,[d] Celso Vataru Nakamura,[d] Luiz Carlos Alves,[ef] Fábio André Brayner,[ef] Ana Cristina Lima Leite*[b] and Tashfeen Akhtar*[a]

Chagas and leishmaniasis are both neglected tropical diseases, whose inefficient therapies have made them remain the cause for millions of deaths worldwide. Given this, we synthesized 27 novel 1,3-thiazoles and 4-thiazolidinones using bioisosteric and esterification strategies to develop improved and safer drug candidates. After an easy, rapid and low-cost synthesis with satisfactory yields, compounds were structurally characterized. Then, *in vitro* assays were performed, against *Leishmania infantum* and *Leishmania amazonensis* promastigotes, *Trypanosoma cruzi* trypomastigotes and amastigotes, for selected compounds to determine IC_{50} and SI, with cytotoxicity on LLC-MK2 cell lines. Overall, 1,3-thiazoles exhibited better trypanocidal activity than 4-thiazolidinones. The compound **1f**, an *ortho*-bromobenzylidene-substituted 1,3-thiazole (IC_{50} = 0.83 μM), is the most potent of them all. In addition, compounds had negligible cytotoxicity in mammalian cells (CC_{50} values > 50 μM). Also noteworthy is the examination of the cell death mechanism of *T. cruzi*, which showed that compound **1f** induced necrosis and apoptosis in the parasite. Scanning electron microscopy analysis demonstrated that the treatment of *Trypanosoma cruzi* trypomastigote cells with the compound **1f** at different IC_{50} concentrations promoted alterations in the shape, flagella and body surface, inducing parasite death. Together, our data revealed a novel series of 1,3-thiazole structure-based compounds with promising activity against *Trypanosoma cruzi* and *Leishmania* spp., broadening ways for scaffold optimization.

Received 14th August 2020
Accepted 25th October 2020

DOI: 10.1039/d0ra06994a

rsc.li/rsc-advances

Introduction

Leishmaniasis consists of a group of diseases caused by the *Leishmania* protozoan, a component of the Trypanosomatidae family, which also includes *Trypanosoma cruzi*, the etiological agent of chagas disease. Beyond other characteristics, they have the presence of differentiated mitochondria called kinetoplastid in common.[1] They are so-called Neglected Tropical Diseases (NTDs) due to various characteristics regarding their occurrence, to be noted poor housing conditions, lack of an adequate sanitary system, treatment, control scheme, malnutrition and scarce resources for investment in research.[2]

The current therapy of chagas disease is mainly based on two compounds, Nifurtimox (**NFX**) and Benznidazole (**BZD**), which were developed about 40 years ago,[3] and are associated with long-term treatments, severe side effects and low access worldwide.[4,5] In fact, **NFX** and **BZD** can eliminate latent parasitemia and reduce serological titers in acute and early chronic infections.[6,7] However, they have low efficacy in prolonged chronic infections.[8]

The treatment of choice for leishmaniasis has been based on pentavalent antimonials.[9] The second line treatment of chagas disease includes drugs, such as Amphotericin B, Pentamidine and Miltefosine.[10] Most treatments are inadequate, owing to factors like a low therapeutic index, which leads to high toxicity and side effects, the emergence of resistant parasites, high costs beyond the means of the affected countries and others. These disadvantages, together with the lack of an effective vaccine, indicate the need to investigate new drugs for NTDs.[10]

[a]*Department of Chemistry, Mirpur University of Science and Technology (MUST), Mirpur, Allama Iqbal Road, 10250-Mirpur, AJK, Pakistan. E-mail: tashfeenchem@must.edu.pk*

[b]*Laboratório de Planejamento em química medicinal, Department of Pharmaceutical Sciences, Health Sciences Centre, Federal University of Pernambuco, 50740-520, Recife, PE, Brazil. E-mail: acllb2003@yahoo.com.br*

[c]*Aggeu Magalhães Research Center, Fundação Oswaldo Cruz, 50670-420, Recife, PE, Brazil*

[d]*Laboratório de Inovação Tecnológica no Desenvolvimento de Fármacos e Cosméticos, State University of Maringá, Paraná, Brazil*

[e]*Laboratório de Imunopatologia Keizo Asami (LIKA), Campus UFPE, 50670-901, Recife, PE, Brazil*

[f]*Instituto Aggeu Magalhães, Fundação Oswaldo Cruz, 50670-420, Recife, PE, Brazil*

Drug discovery approaches, for NTDs such as the aforementioned ones, have been a hot topic in medicinal chemistry in the last years since their last annual occurrence was of more than 1 billion people with significant mortality of 500 000,[11] calling for urgent attention to this topic.

Considering the lack of effective, affordable, or easy-to-use drug treatments for NTDs, the adoption of the Privileged Structures strategy has been advantageous to provide new chemical entities with good 'drug-like' properties. Privileged motifs are recurring in a wide range of biologically active compounds that reach different pharmaceutical targets and pathways. The drug-like properties of privileged structures and substructures might produce many drug-like compound libraries and leads.[12,13]

For example, 1,3-thiazole and 4-thiazolidinone nuclei are privileged structures that are found in several natural products, and have also been used to develop synthetic drugs and drug-like molecules with a variety of pharmacological effects.[14–22]

Taking account of their biological diversity and potential, together with the easy and rapid synthesis, 4-thiazolidinones and 1,3-thiazoles are outlined scaffolds in medicinal chemistry. A good strategy for optimizing bioactive compounds is the bioisosterism. This approach has been considered efficient through thiosemicarbazones cyclization to 1,3-thiazoles/4-thiazolidinones, taking to anti-*T. cruzi* and anti-*Leishmania* spp. activity enhancement.[23–26]

Indeed, we have used the bioisosteric strategy on previously synthesized compounds by our group. The thiosemicarbazones cyclization to 4-thiazolidinones obtained 23 different bioactive 4-oxo-thiazolidinones-5-acetic-acids. As a common structural feature, this series of compounds presented an acetic acid in the 5th position of the 4-oxo-thiazolidinones ring system, and a varied ring core at the hydrazone moiety. Some of these reported compounds showed potent trypanocidal activity and low toxicity to mammalian cells.[27]

Herein, we present two novel series, exploring the bioisosteric strategy on thiosemicarbazones cyclization to 1,3-thiazoles/4-thiazolidinones rings and developing a novel derivatives from the carboxylic acids produced by our group.[27] The hypothesis was based on the concept of whether the classical medicinal chemistry using esterification could be used to simultaneously improve the solubility and permeability to obtain acetates. In two different series, we used a simple two-step synthesis approach to obtain novel 1,3-thiazoles (**1a–k**) and 4-thiazolidinones (**2a–p**) from the thiosemicarbazones nucleus, as summarized in Fig. 1. Following the synthesis, we characterized these molecules and evaluated their trypanocidal, leishmanicidal and cytotoxic activities. The utmost promising molecule was chosen to assess necrosis development on trypomastigotes by flow cytometry assay and evaluation of activity against the intracellular forms of *T. cruzi*, as well as evaluation of its ultrastructural impacts on *T. cruzi* trypomastigotes, seen by scanning electron microscopy (SEM). All data were collected to establish the structure–activity relationships (SAR), and provide a comparison with the previous results of their bioisosteric analogues[27] and reference drugs. Hence, our work demonstrates that 1,3-thiazoles and 4-thiazolidinone acetates are a versatile building block for lead generation, easily yielding access to diverse derivatives for drug optimization.

Results and discussion

Chemistry

1,3-Thiazoles synthesis and characterization. Firstly, ethyl 2-(2-(arylidene)hydrazinyl)thiazole-4-carboxylates (**1a–k**) were synthesized, as shown in Scheme 1. Different substituted

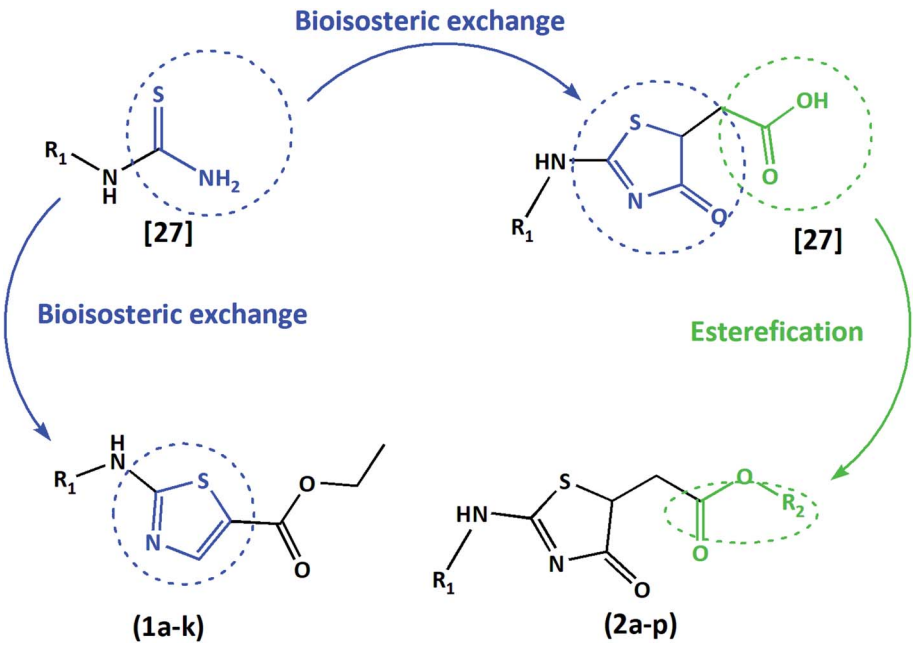

Fig. 1 Summary of the structural planning of the novel 1,3-thiazoles and 4-thiazolidinones reported in this work, based on previous results.[27]

aldehydes were condensed with thiosemicarbazide *via* Schiff base condensation to obtain respective thiosemicarbazones, as in our previous work.[26] The thiosemicarbazones were then cyclized to their respective 1,3-thiazole-4-carboxylates (**1a–k**) with ethyl bromopyruvate using absolute ethanol under reflux for about 4–6 hours. After reflux, the solids were precipitated when put on ice. The products were obtained with satisfactory yields, ranging from 73% to 90%. Only compounds **1d** (51%) and **1g** (61%) had lower yields, with the possibility of optimization. The purity of all compounds was ascertained by observing a single spot on TLC. The synthesized ethyl 2-(2-(arylidene)hydrazinyl)thiazole-4-carboxylates were initially characterized by observing changes in their physical parameters relating to the color, retardation factor (R_f), and melting point values. The compounds **1a–k** were further verified and confirmed by different spectroscopic techniques. FT-IR, ^{1}H-, ^{13}C-NMR and high-resolution mass spectrometry results revealed that the proposed structures of the synthesized 1,3-thiazoles were in good agreement with the actual structures. In FT-IR, a carbonyl group stretching was observed within the range of 1699–1724 cm^{-1}. In the ^{1}H-NMR spectra, three protons triplet of –CH_3 and two protons quartet of –CH_2– were observed around 1.26–1.28 ppm and 4.22–4.28 ppm, respectively, and were assigned to the ethyl group of the ester moiety. One proton singlet appeared at 7.73–7.79 ppm, and was assigned to the proton of the thiazole ring. The multiplicity of the aromatic protons appeared at their respective position in the aromatic region with regards to the substitution patterns. In the ^{13}C-NMR spectra, two carbon signals upfield at around 14.2–14.6 and 60.8–60.9 ppm were assigned to the ethyl group of the ester moiety. The formation of the synthesized 1,3-thiazole-4-carboxylates was confirmed by high-resolution mass spectrometry technique.

4-Thiazolidinones synthesis and characterization. To produce our second series of compounds, we used the esterification strategy of preceding acetic acids published by our group[26] in novel alkyl 2-((2-(arylidene)hydrazinyl)-4-oxo-4,5-dihydrothiazol-5-yl)acetates (**2a–p**), which were synthesized as shown in Scheme 2. The 4-oxothiazolidine-5-acetic acids were then esterified using thionyl chloride and the respective alcohol. After almost one hour of reflux, a solid precipitated when the reaction mixture was poured onto ice. The synthesized **2a–p** were characterized, and confirmed by physical parameters analysis and different spectroscopic techniques. In FT-IR, the characteristic alkyl chain –CH_2– stretching was observed at 2981–3093 cm^{-1}. In the ^{1}H-NMR spectra, three protons triplet at 1.17–1.19 ppm and two protons quartet at 4.03–4.17 ppm due to –CH_3 and –OCH_2–, respectively, were assigned to the ethyl group of the ester moiety, verifying the successful esterification of the 2-(2-(arylidene) hydrazono)-4-oxothiazolidine-5-acetic acids. The aromatic and other protons appeared in their respective regions, depending on their substitution patterns. In the ^{13}C-NMR spectra, carbon signals observed at the upfield region around 14.4–14.6 and 60.8–61.2 ppm, and were assigned to the ethyl carbons of the ester moiety. The structures of the synthesized 4-thiazolidinones were further confirmed by mass spectrometry techniques.

Cytotoxic studies

The potential cytotoxic profile of novel compounds against mammalian cells was investigated by MTT assay[28] using LLC-MK2

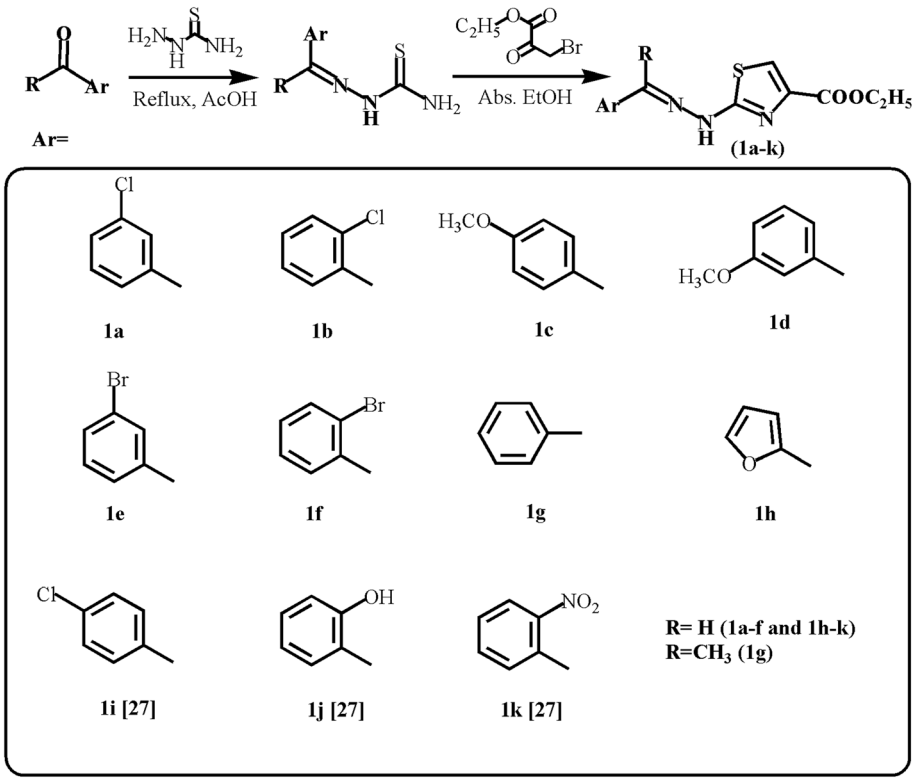

Scheme 1 Synthetic route for ethyl 2-(2-(arylidene)hydrazinyl)thiazole-4-carboxylates (**1a–h**; **1i–k**[27]).

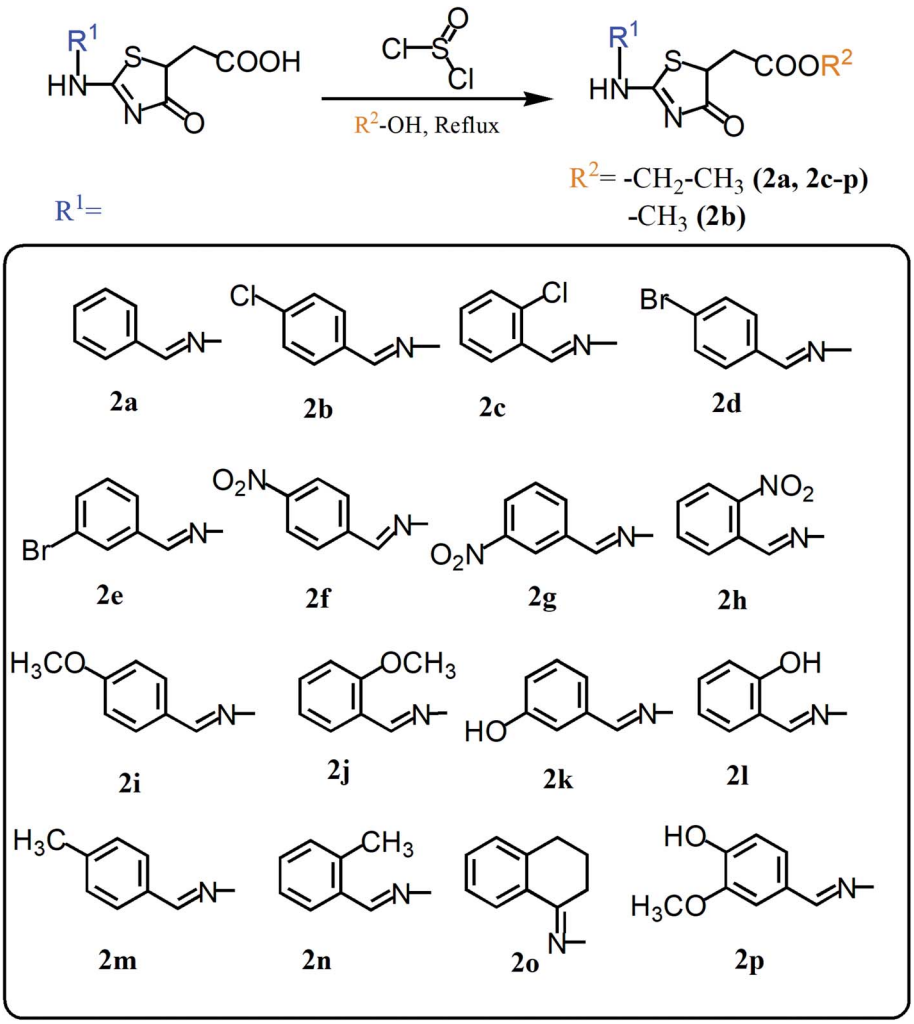

Scheme 2 Synthetic route for alkyl 2-((2-(arylidene)hydrazinyl)-4-oxo-4,5-dihydrothiazol-5-yl)acetate (**2a–p**).

cells. Compounds **1a–k** and **2a–p** were added in increasing concentrations (10 to 1000 μM), and incubated for 96 hours for the determination of the 50% cytotoxic concentration (CC_{50}). As we can see in Table 1, no compounds were considered cytotoxic to mammalian cells since all of the CC_{50} values were higher than 50 μM. However, compounds **1d**, **1j**, **1k**, **2b** and **2n** exhibited higher CC_{50} values than the reference **BZD** with highlights to the *o*-methyl substituted **2n** (CC_{50} = 770.37; SI_{Trypo} = 61) and the *p*-methyl substituted **2b** (CC_{50} = 659.08; $SI_{L.inf}$ = 19.8) being less cytotoxic.

Trypanocidal activity evaluated against trypomastigote form

The compounds **1a–k** and **2a–p** were evaluated *in vitro* against *T. cruzi* trypomastigote (strain Y). As shown in Table 1, most of the tested compounds showed a promising IC_{50} value and selectivity in comparison to the reference drug, **BZD** (IC_{50} = 34.5 μM and SI = 17.8). The compounds that had outstanding performance with minimal inhibitory concentration for 50% of the parasite cells (less than 10 μM) were **1f**, **1h**, **1g**, **1a** and **2d** (0.83 μM, 2.75 μM, 2.83 μM, 4.44 μM and 8.45 μM, respectively). The synthesized compounds **1h** (a furan moiety derivative), **1g** (benzylidene) and **1a** (*m*-Cl-benzylidene) were over a hundred times more selective to *T. cruzi* than to the mammalian cells (SI = 153.6, 103.3 and 121.2, respectively), outlining **1f** (*o*-Br-benzylidene) that performed a selectivity of 303.2 in comparison with 17.8 of **BZD**. Concerning the 4-thiazolidinones derivatives, it was verified that among the **2a–p** series, compound **2d** exhibited the best IC_{50} value (8.45 μM). Regarding the selectivity index, we can highlight that compound **2d** (*p*-Br-benzylidene, SI = 47), **2e** (*m*-Br-benzylidene, SI = 24.2), **2i** (*p*-CH_3O-benzylidene, SI = 31.4), **2j** (*o*-CH_3O-benzylidene, SI = 22.3), **2m** (*p*-CH_3-benzylidene, SI = 20.8), and **2n** (*o*-CH_3-benzylidene, SI = 61), with **2p** (*m*-methoxy and *p*-hydroxy benzylidene, SI = 15.3) performed better than **BZD**. The methyl substitution on the aromatic ring was evidenced as a good change, resulting in satisfactory IC_{50} values in both synthesized positions (*ortho* and *para*), as well as the methoxy substitution. In addition, the two leading compounds were *ortho*-substituted in terms of the trypanocidal activity of both series, evidencing the importance of this position and corroborating our previous results with the non-cyclized **1g*** (IC_{50} = 5.65 μM),[27] which presents an *o*-chlorine substitution.

In general, the 1,3-thiazole derivatives (**1a–k**) were more effective than the 4-thiazolidinones (**2a–p**) ones. The compounds **1f** and **1h** can be highlighted as the hit compounds,

Table 1 Determination of the *in vitro* cytotoxic, trypanocidal and leishmanicidal activity of **1a–k** and **2a–p** derivatives in comparison with the standard drugs **BZD**[28] and Miltefosine[29d]

		Trypomastigotes		Promastigotes			
				IC_{50}[b] (μM)		SI[c]	
Compound code	LLC-MK2, CC_{50}[a] (μM)	EC_{50}[b] (μM)	SI[c]	$IC_{50L.Ama}$	$IC_{50L.Inf}$	$SI_{L.Ama}$	$SI_{L.Inf}$
1a	538.34	4.44	121.2	189.27	164.32	2.8	3.3
1b	258.4	12.50	20.7	27.89	14.39	9.3	18.0
1c	>1000	20.51	>48.8	391.68	332.08	2.6	3.0
1d	640.79	12.91	15.5	159.19	103.85	4.0	6.2
1e	600.46	46.73	12.8	245.55	170.28	2.4	3.5
1f	251.66	0.83	303.2	24.34	23.46	10.3	10.7
1g	292.4	2.83	103.3	42.96	37.43	6.8	7.8
1h	422.4	2.75	153.6	451.2	374.16	0.9	1.1
1i	598.56	24.87	24.1	145.07	108.11	4.1	5.5
1j	926.07	ND	NA	484.67	289.74	1.9	3.2
1k	661.54	ND	NA	359.02	158.9	1.8	4.2
2a	471.36	33.83	13.9	366.79	365.48	1.3	1.3
2b	659.08	ND	NA	91.35	33.24	7.2	19.8
2c	229.11	ND	NA	113.86	128.72	2.0	1.8
2d	397.45	8.45	47.0	14.63	14.49	27.2	27.4
2e	445.76	18.24	24.4	119.76	115.55	3.7	3.9
2f	722.89	ND	NA	57.5	324.99	12.6	2.2
2g	430.47	ND	NA	308.54	329.38	1.4	1.3
2h	577.05	ND	NA	17.01	295.13	33.9	2.0
2i	399.41	12.72	31.4	169.44	146.52	2.4	2.7
2j	538.62	24.15	22.3	185.58	236.03	2.9	2.3
2k	613.59	ND	NA	363.77	370.31	1.7	1.7
2l	53.45	19.76	2.7	84.3	67.27	0.6	0.8
2m	609.45	29.26	20.8	13.35	18.82	45.7	32.4
2n	770.37	12.62	61.0	267.54	167.85	2.9	4.6
2o	279.57	27.87	10.0	179.75	176.27	1.6	1.6
2p	544.65	35.49	15.3	232.76	320.16	2.3	1.7
BZD[10]	614.7	34.5 ± 7.6	17.8	NA	NA	NA	NA
Miltefosine[29]	12.27	NA	NA	36.31	53.71	0.3	0.2

[a] CC_{50} = cytotoxic concentration for 50% of the cells. [b] EC_{50} = effective concentration for 50% of the parasites. [c] SI = selectivity index (CC_{50}/IC_{50}). [d] NA = non-applicable; ND = no difference.

given their enhanced trypanocidal activity with high selectivity to parasite cells, and the low concentrations needed to kill half of the parasite population, with **1f** at the nanomolar scale (830 nM).

Trypanocidal activity evaluated against the amastigote forms

The compounds **1a**, **1g**, **1h** and **1f** were tested in six different concentrations (0.625, 1.25, 2.5, 5, 10 and 20 μg mL^{-1}) against *T. cruzi* amastigotes (Tulahuen strain). The analysis of the obtained results, displayed in Table 2, indicate that compound **1a** was the best among the tested compounds, with an IC_{50} = 16.85 μM and SI = 31.9. Nevertheless, it was weaker than the standard drug **BZD** (IC_{50} = 5.65 μM, SI = 108.8).

Cell death assessment

After the outstanding trypanocidal activity, the cell death mechanism rates of the nanomolar-active compound **1f** was investigated using **BZD** as a standard. This was assessed through conventional staining with Propidium Iodide (PI) and Annexin-V in the flow cytometry method. First, PI is a stain that passes

Table 2 Results of the trypanocidal activity evaluation of compounds **1a**, **1g**, **1h**, **1f** and **BZD** against the amastigote forms of the Tulahuen strain of *Trypanosoma cruzi*. Negative control—RPMI-1640 medium plus 1% DMSO displayed 0% lysis

Compound code	LLC-MK2, CC_{50}[a] (μM)	Amastigote, IC_{50}[b] (μM)	Amastigote, SI[c]
1a	538.34	16.85	31.9
1g	292.4	40.71	7.2
1h	422.4	75.39	5.6
1f	251.66	56.46	4.5
BZD	614.7	5.65	108.8

[a] CC_{50} = cytotoxic concentration for 50% of cells. [b] IC_{50} = inhibitory concentration for 50% of cells. [c] SI = selectivity index (CC_{50}/IC_{50}).

within the cell membrane whenever it is damaged, reaching and binding directly to the DNA. On the other hand, Annexin V binds to the phospholipid phosphatidylserine that is found in the inner side of the cell membrane. There, it stains whenever this phospholipid is exposed, which happens when the cells go through the apoptosis process. Moreover, when the apoptotic process is late or involves necrosis, there is PI staining on DNA.[31]

As shown in Fig. 2, compound **1f** (at 1.66 μM and 3.32 μM) was able to induce significant labeling, which is consistent with necrosis in trypomastigotes. Similar results were found in parasites treated with **BZD** (34.5 μM, 70.8 μM, and 141.6 μM), the reference drug, and the positive control used in this assay (Fig. 2A). Furthermore, at 3.32 μM concentration of **1f**, an equivalent necrosis was observed (17.58% double-stained) as that for the 70.8 μM of **BZD** (19.56% double-stained), reinforcing the potency of the 1,3-thiazole derivatives in comparison with the standard drug (Fig. 2B).

Ultrastructural studies for *T. cruzi*

To evaluate the effects of 1,3-thiazoles on the parasite morphology, the most active compound of this work (**1f**) was selected. Scanning electron microscopy analysis (Fig. 3) showed that *T. cruzi* trypomastigotes in the control group had preserved morphologies in the body and flagella (Fig. 3A), while cells treated with **BZD** had their bodies contorted with the extravasation of cytoplasmic content (Fig. 3B). In contrast, cells treated with **1f** at IC_{50}, 2 × IC_{50}, and 4 × IC_{50} (0.8 μM, 1.66 μM and 3.32 μM) concentrations, respectively, promoted dose-dependent alterations in the shape, flagella and surface of the parasite's body (Fig. 3C–E) when compared to the untreated control group. Furthermore, the compound **1f** promoted body writhing with a swollen and rounded appearance, shortening of the flagellum, plus a disruption of the membrane with extravasation of the cytoplasmic content. The activity of compound **1f** can be observed through ultrastructural alterations caused in *T. cruzi*, which certainly makes the cell unfeasible.

Leishmanicidal activity evaluated against promastigote forms

The ability of the new derivatives (**1a–k** and **2a–p**) to inhibit the growth of the promastigote forms of *L. amazonensis* and *L. infantum* was investigated using Miltefosine as a standard.[30] It was verified that all of the synthesized compounds were less

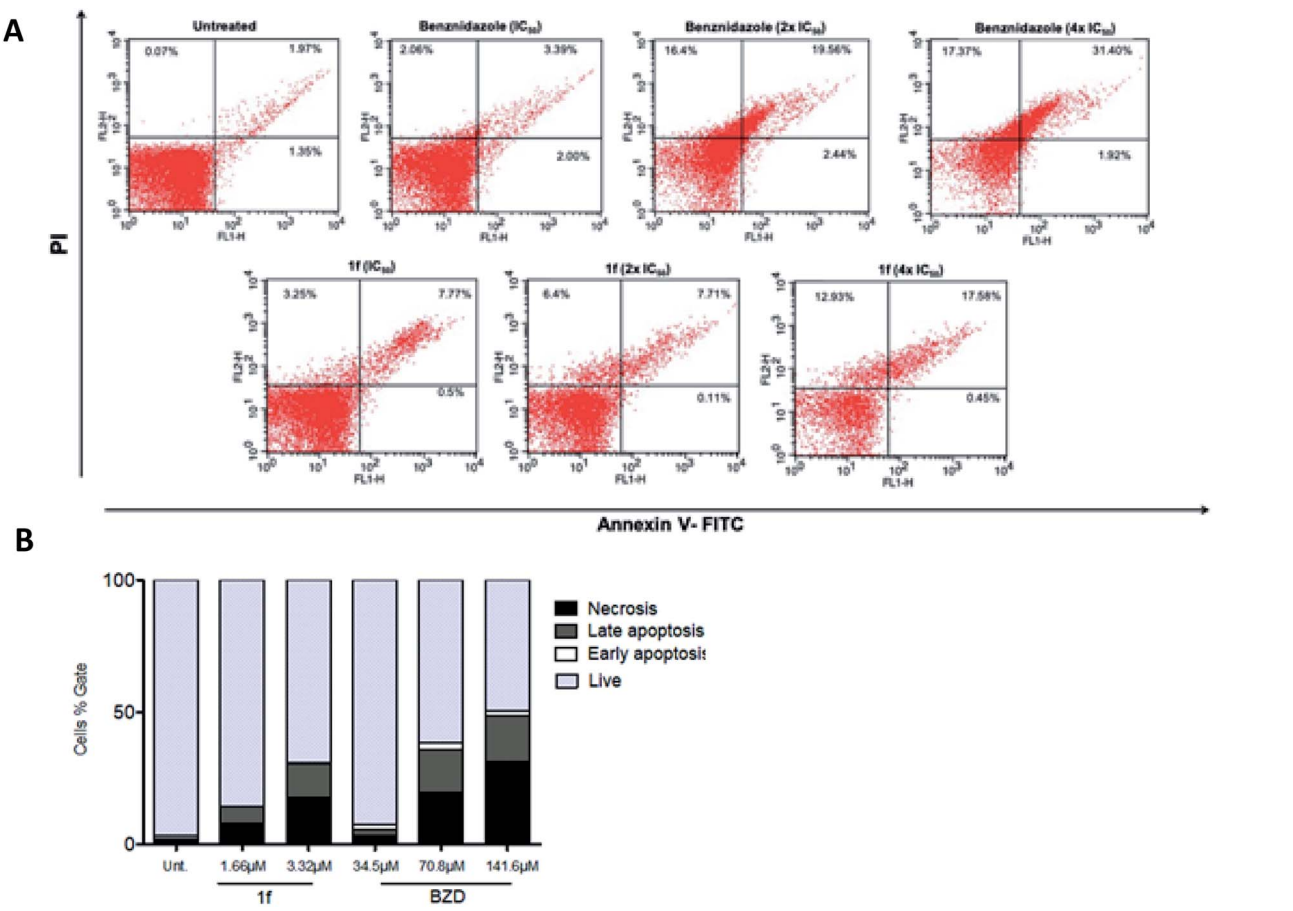

Fig. 2 Flow cytometry results on *T. cruzi* trypomastigotes untreated and treated with **1f** at 2 × IC_{50} (1.66 μM) and 4 × IC_{50} (3.32 μM); and treated with **BZD** at 1 × IC_{50} (34.5 μM), 2 × IC_{50} (70.8 μM), and 4 × IC_{50} (141.6 μM), following staining with PI and Annexin-V. (A) Plotted flow cytometry graphs with FITC on the *X*-axis and PI on the *Y*-axis. (B) Bar chart illustrating the proportions of each cell death mechanism among all concentrations of **1f** and **BZD** tested, and comparison with the untreated group. The percentage of populations can be separated on double-negative (live) cells, Annexin-V positive (early apoptotic cells), PI-positive (late apoptotic), and double-positive (necroptotic) cells. All *p* values of the shown concentrations were below 0.05. The graphs were plotted with the GraphPad Prism ® software.

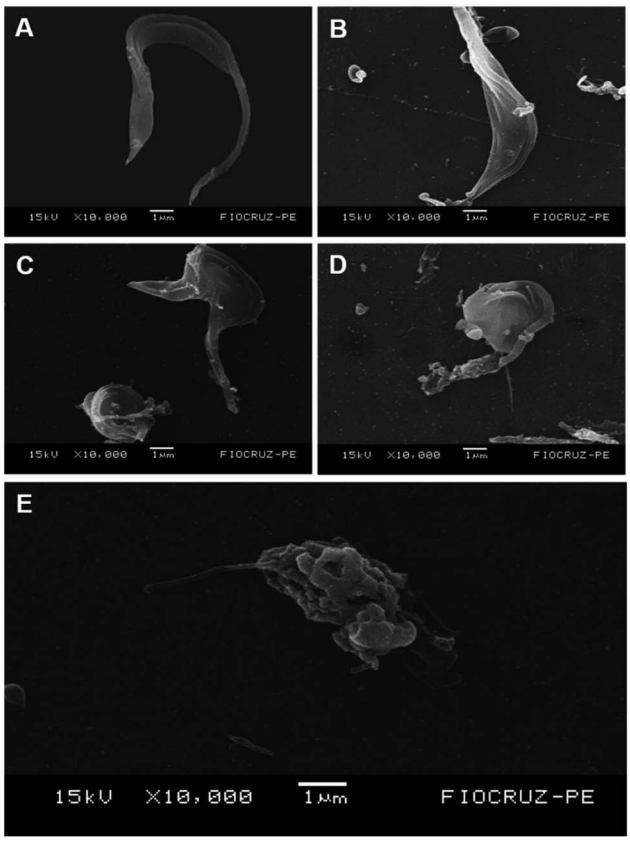

Fig. 3 Ultrastructural alterations in trypomastigote forms of *T. cruzi* treated with BZD and compound **1f** by SEM. (A) Control untreated trypomastigotes showing the typical elongated body with the slick cell surface and preserved flagellum. (B) Treated trypomastigotes with BZD (IC_{50} = 34.5 µM) showing a contorted and swollen body, with disruption displaying internal cell content. (C) Treated trypomastigotes with **1f** (IC_{50} = 0.8 µM) showing body writhed with appearance swollen and rounded, beyond flagellum shortening. (D) Treated trypomastigotes with **1f** (2 × IC_{50} = 1.66 µM), showing a rounded body, rupture of the cytoplasmic membrane, and exposure of internal cellular content. (E) Treated trypomastigotes with **1f** (4 × IC_{50} = 3.32 µM) showing alterations in the flagella form and cell body, with total membrane destruction and extravasation of the cytoplasmic content.

toxic and more selective than the standard drug Miltefosine, as shown in Table 1.

The compounds **1b**, **1f**, **2d** and **2m** exhibited better IC_{50} values for both *L. amazonensis* (27.89 µM, 23.34 µM, 14.63 µM and 13.35 µM) and *L. infantum* (14.39 µM, 23.46 µM, 14.49 µM and 18.81 µM), in comparison to the standard Miltefosine (36.31 µM and 53.71 µM). They also displayed good selectivity, with a focus on **2d** (around 27 times, both) and **2m** (SI = 45.7 and SI = 32.4) that had high SI for both *Leishmania* spp. tested. In addition, **2m** performed the highest selectivity value for *L. amazonensis* of all tested compounds, being 46 times more selective to the parasite than to the LLC-MK2 cells (and 32.4 to *L. infantum*). Among the 1,3-thiazoles, the compound **1f** was once again evidenced for its bioactivity (*L. amazonensis* – IC_{50} = 24.34 µM, SI = 10.3; *L. infantum* – IC_{50} = 23.46 µM, SI = 10.7), together with **1g** (*L. infantum* – IC_{50} = 37.43 µM, SI = 7.8) and **1b** (*L. amazonensis* – IC_{50} = 27.89 µM, SI = 9.3; *L. infantum* – IC_{50} = 14.39 µM, SI = 18). Furthermore, the *ortho*-substitution with a halogen group on the benzylidene moiety was demonstrated to be beneficial for the bioactivity of the substituted 1,3-thiazole-4-carboxylates, whereas the 4-thiazolidinone-5-acetates displayed enhanced leishmanicidal activity when *para*-substituted (**2m**, **2d**, **2b**). In addition, the compound **2d** (*p*-Br-benzylidene) is outlined as a promising structure with satisfactory activity against both *T. cruzi* (SI = 47) and *Leishmania* sp. ($SI_{L.ama}$ = 27.2; $SI_{L.inf}$ = 27.4), having the same atom allocated on the benzylidene ring as **1f** (*o*-bromine). Moreover, our strategy of esterification was proven to be efficient since the outstanding carboxylic acids synthesized by our group had their activity greatly improved, to enumerate: **1b*** ($IC_{50L.ama}$ = 34.48 µM, $IC_{50L.inf}$ = 59.52 µM) *p*-bromine substituted that was esterified to **2d**, and **1c*** ($IC_{50L.inf}$ = 85.30 µM), *p*-chlorine that originated from **2b**.[27]

The summarized SAR evaluation for both 1,3-thiazoles and 4-thiazolidinones can be seen in Fig. 4, while the trypanocidal and leishmanicidal activities regarding the SI values are compiled in Fig. 5.

Experimental

Synthesis and characterization of novel 1,3-thiazole and thiazolidin-4-one analogues

High-purity grade reagents and solvents were used for the synthesis of ethyl 2-(2-(arylidene)hydrazinyl)thiazole-4-carboxylates (**1a–k**) and alkyl 2-((2-(arylidene)hydrazinyl)-4-oxo-4,5-dihydrothiazol-5-yl)acetates (**2a–p**). All synthesized esters of 1,3-thiazoles and thiazolidin-4-ones were initially characterized by their physical parameters, like the change in color,

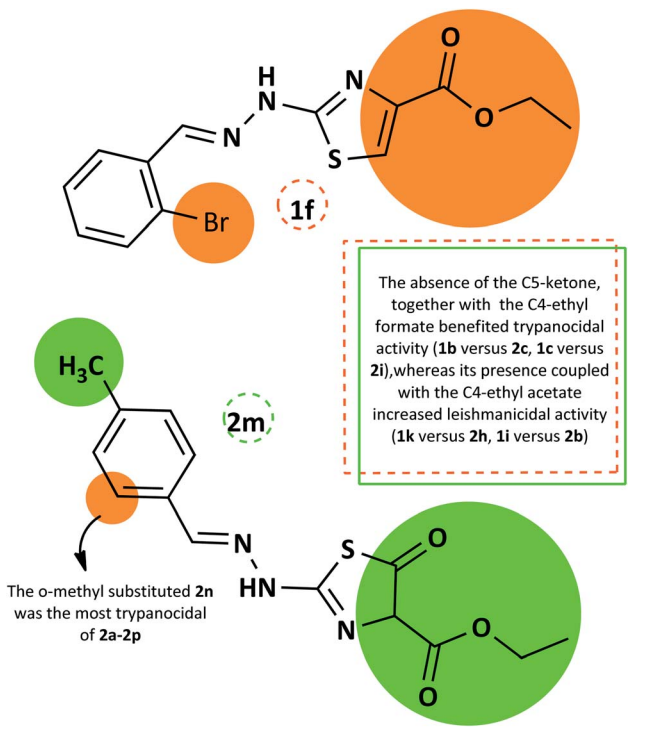

Fig. 4 Summary of the SAR evaluation between the top compounds of each 1,3-thiazole series (**1f**) and 4-thiazolidinone series (**2m**), regarding the trypanocidal and leishmanicidal activity.

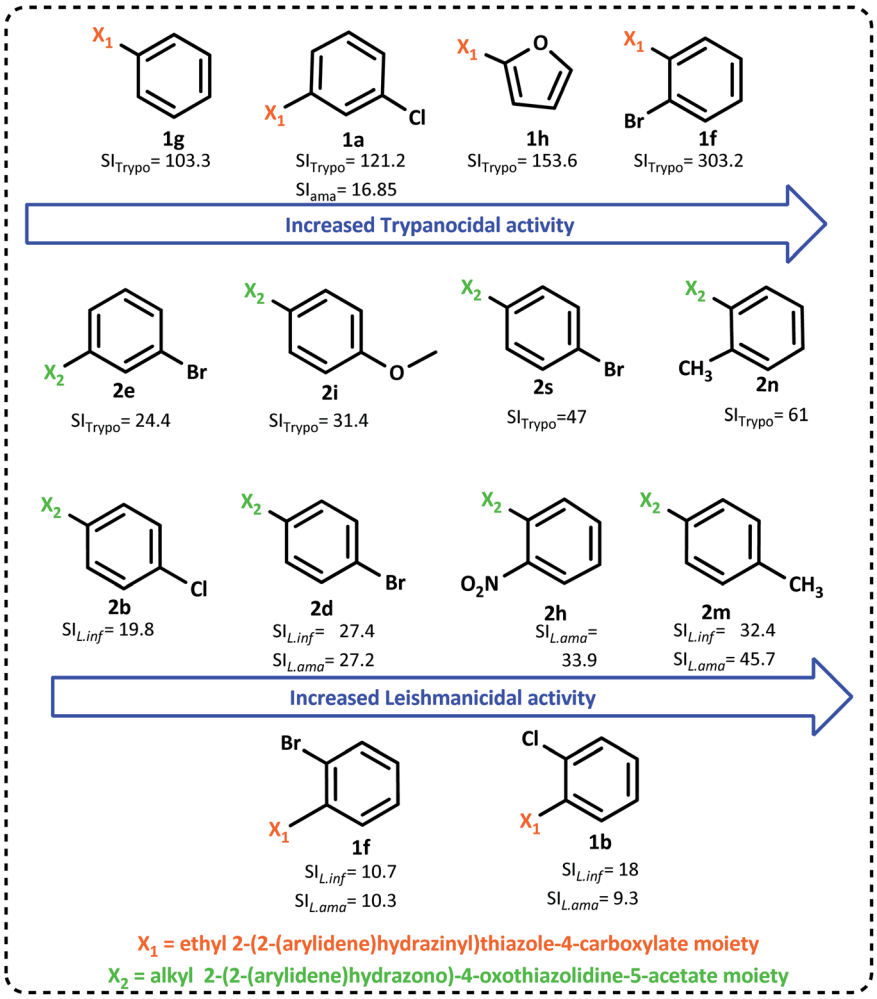

Fig. 5 Improvement in the SI (selectivity index) values was observed by the change in the radicals of 1,3-thiazoles and 4-thiazolidinones.

melting points, and the R_f (retardation factor) values. Spectroscopic techniques, like FT-IR, NMR and high-resolution mass spectrometry, were used for the confirmation of the synthesized compounds. To evaluate the purity of all synthesized compounds, the R_f values were calculated by thin-layer chromatography using silica gel 60 HF254 pre-coated aluminum sheets (Merck). Melting points were recorded on DMP-300 A&E Lab UK, apparatus. Characteristic functional groups were determined by the FT-IR spectrophotometer using ATR. Bruker 300 MHz, Varian VNMRS 400 MHz, and 500 MHz spectrometers were used to check protons and carbon signals. HRMS was recorded using a MALDI-TOF mass spectrometer, Bruker. The purity of the selected compound was calculated by qualitative HNMR method using qHNMR normalization (100%) method, established by Pauli *et al.* The spectra were recorded using this optimized protocol.[32]

Synthesis and characterization of ethyl 2-(2-(arylidene) hydrazinyl)thiazole-4-carboxylates (1a–k)

Different aryl-substituted thiosemicarbazones (1.0 mmol) and ethyl bromopyruvate (1 : 1 equivalent) were refluxed in absolute ethanol for 4 to 6 hours. Thin-layer chromatography (TLC, acetone : *n*-hexane; 1 : 2) was used to check the completion and purity of the reaction. The reaction mixture solidified when put on ice. The solid was filtered and washed with plenty of water to obtain a pure product, and dried at room temperature.

Ethyl 2-(2-(3-chlorobenzylidene)hydrazinyl)thiazole-4-carboxylate (1a). Light yellow solid; yield: 89%; melting point: 249–251 °C; R_f: 0.54 (acetone/*n*-hexane, 1 : 2); IR (ATR, cm^{-1}): 1093 (C–O stretching, ester), 1446 (C–H bending, aliphatic), 1573 (C=C ring stretching), 1716 (C=O stretching), 2987 (C–H stretching, aliphatic); ^{1}H-NMR (300 MHz): δ 1.28 (3H, t, –CH$_3$ ester, J = 7.20 Hz), 4.25 (2H, q, –CH$_2$–CH$_3$ ester, J = 7.20 Hz), 7.44 (2H, m, Ar-H), 7.61 (1H, m, Ar-H), 7.70 (1H, m, Ar-H), 7.78 (1H, s, 1,3-thiazole ring C-5), 7.90 (1H, s, –CH=N- azomethine), 12.49 (1H, s, –N–NH–C–); ^{13}C-NMR (75 MHz): δ 14.6 (–CH$_3$ ester), 60.9 (–OCH$_2$– ester), 119.7 (1,3-thiazole ring C-5), 125.5, 126.1, 129.5, 131.2, 134.2, 136.9 (Ar-C), 140.6 (–CH=N– azomethine), 143.6 (1,3-thiazole ring C-4), 161.4 (C=O), 168.4 (1,3-thiazole ring C-2); HRMS (MALDI-TOF): calcd $C_{13}H_{12}ClN_3NaO_2S$ (M + Na) = 332.02364, found: 332.01055.

Ethyl 2-(2-(2-chlorobenzylidene)hydrazinyl)thiazole-4-carboxylate (1b). Off white solid; yield: 90%; melting point:

213–215 °C; R_f: 0.60 (acetone/*n*-hexane, 1 : 2); IR (ATR, cm^{-1}): 1091 (C–O stretching, ester), 1423 (C–H bending, aliphatic), 1585 (C=C ring stretching), 1687 (C=N stretching), 1724 (C=O stretching), 2985 (C–H stretching, aliphatic); ^{1}H-NMR (300 MHz): δ 1.27 (3H, t, –CH_3 ester, J = 7.20 Hz), 4.28 (2H, q, –CH_2–CH_3 ester, J = 7.20 Hz), 7.39 (2H, m, Ar-H), 7.47 (1H, m, Ar-H), 7.79 (1H, s, 1,3-thiazole ring C-5), 7.90 (1H, m, Ar-H), 8.34 (1H, s, –CH=N– azomethine), 12.48 (1H, s, –N–NH–C–); ^{13}C-NMR (75 MHz): δ 14.6 (–CH_3 ester), 60.9 (–OCH_2– ester), 119.8 (1,3-thiazole ring C-5), 126.7, 128.1, 130.4, 131.3, 131.8, 132.7 (Ar-C), 138.0 (–CH=N– azomethine), 143.3 (1,3-thiazole ring C-4), 161.4 (C=O), 168.3 (1,3-thiazole ring C-2); HRMS (MALDI-TOF): calcd $C_{13}H_{12}ClN_3NaO_2S$ (M + Na) = 332.02364, found: 331.99641.

Ethyl 2-(2-(4-methoxybenzylidene)hydrazinyl)thiazole-4-carboxylate (1c). Yellowish brown solid; yield: 80%; melting point: 213–215 °C; R_f: 0.58 (acetone/*n*-hexane, 1 : 2); IR (ATR, cm^{-1}): 1091 (C–O stretching, ester), 1423 (C–H bending, aliphatic), 1585 (C=C ring stretching), 1687 (C=N stretching), 1724 (C=O stretching), 2985 (C–H stretching, aliphatic); ^{1}H-NMR (300 MHz): δ 1.28 (3H, t, –CH_3 ester, J = 7.20 Hz), 3.79 (3H, s, –OCH_3), 4.23 (2H, q, –CH_2–CH_3 ester, J = 7.20 Hz), 6.99 (2H, d, Ar-H, J = 8.70 Hz), 7.59 (2H, d, Ar-H, J = 8.70 Hz), 7.73 (1H, s, 1,3-thiazole ring C-5), 7.95 (1H, s, –CH=N– azomethine), 12.14 (1H, s, –N–NH–C–); ^{13}C-NMR (75 MHz): δ 14.6 (–CH_3 ester), 55.7 (–OCH_3), 60.8 (–OCH_2– ester), 119.1 (1,3-thiazole ring C-5), 114.8, 127.2, 128.4, 160.8 (Ar-C), 142.4 (-CH=N- azomethine), 143.3 (1,3-thiazole ring C-4), 161.5 (C=O), 168.7 (1,3-thiazole ring C-2); HRMS (MALDI-TOF): calcd $C_{14}H_{15}N_3NaO_3S$ (M + Na) = 328.0732, found: 327.97609.

Ethyl 2-(2-(3-methoxybenzylidene)hydrazinyl)thiazole-4-carboxylate (1d). Yellowish brown solid; yield: 51%; melting point: 188–190 °C; R_f: 0.60 (acetone/*n*-hexane, 1 : 2); IR (ATR, cm^{-1}): 1071 (C–O stretching, ester), 1456 (C–H bending, aliphatic), 1573 (C=C ring stretching), 1617 (C=N stretching), 1708 (C=O stretching), 2980 (C–H stretching, aliphatic); ^{1}H-NMR (300 MHz): δ 1.28 (3H, t, –CH_3 ester, J = 7.20 Hz), 3.79 (3H, s, –OCH_3), 4.24 (2H, q, –CH_2–CH_3 ester, J = 6.90 Hz), 6.95 (1H, m, Ar-H), 7.22 (2H, m, Ar-H), 7.33 (1H, t, Ar-H, J = 7.80 Hz), 7.76 (1,3-thiazole ring C-5), 7.97 (1H, s, –CH=N– azomethine), 12.34 (1H, s, –N–NH–C–); ^{13}C-NMR (75 MHz): δ 14.6 (–CH_3 ester), 55.5 (–OCH_3), 60.9 (–OCH_2– ester), 119.4 (1,3-thiazole ring C-5), 111.6, 115.8, 119.4, 130.4, 136.0, 159.9 (Ar-C), 142.1 (–CH=N– azomethine), 143.3 (1,3-thiazole ring C-4), 161.5 (C=O), 168.6 (1,3-thiazole ring C-2); HRMS (MALDI-TOF): calcd $C_{14}H_{15}N_3NaO_3S$ (M + Na) = 328.0732, found: 327.96025.

Ethyl 2-(2-(3-bromobenzylidene)hydrazinyl)thiazole-4-carboxylate (1e). Light yellow solid; yield: 88%; melting point: 266–268 °C; R_f: 0.54 (acetone/*n*-hexane, 1 : 2); IR (ATR, cm^{-1}): 1095 (C–O stretching, ester), 1446 (C–H bending, aliphatic), 1579 (C=C ring stretching), 1687 (C=N stretching), 1724 (C=O stretching), 2999 (C–H stretching, aliphatic); ^{1}H-NMR (300 MHz): δ 1.28 (3H, t, –CH_3 ester, J = 7.20 Hz), 4.24 (2H, q, –CH_2–CH_3 ester, J = 7.20 Hz), 7.38 (1H, t, Ar-H, J = 7.80 Hz), 7.56 (1H, d, Ar-H, J = 8.70 Hz), 7.65 (1H, d, Ar-H, J = 7.80 Hz), 7.78 (1H, s, 1,3-thiazole ring C-5), 7.83 (1H, s, Ar-H), 7.96 (1H, s, –CH=N– azomethine), 12.44 (1H, s, –N–NH–C–); ^{13}C-NMR (75 MHz): δ 14.6 (–CH_3 ester), 60.9 (–OCH_2– ester), 119.7 (1,3-thiazole ring C-5), 122.7, 125.8, 128.9, 131.5, 132.4, 137.1 (Ar-C), 140.5 (–CH=N– azomethine), 143.3 (1,3-thiazole ring C-4), 161.41 (C=O), 168.4 (1,3-thiazole ring C-2); HRMS (MALDI-TOF): calcd $C_{13}H_{12}BrN_3NaO_2S$ (M + Na) = 375.97313, found: 376.16224.

Ethyl 2-(2-(2-bromobenzylidene)hydrazinyl)thiazole-4-carboxylate (1f). Light yellow solid; yield: 81%; melting point: 226–228 °C; R_f: 0.59 (acetone/*n*-hexane, 1 : 2); IR (ATR, cm^{-1}): 1103 (C–O stretching, ester), 1431 (C–H bending, aliphatic), 1575 (C=C ring stretching), 1687 (C=N stretching), 1699 (C=O stretching), 3045 (C–H stretching, aliphatic); ^{1}H-NMR (300 MHz): δ 1.27 (3H, t, –CH_3 ester, J = 7.09 Hz), 4.23 (2H, q, –CH_2–CH_3 ester, J = 7.10 Hz), 7.30 (1H, ddd, Ar-H, J = 1.72 Hz, J = 7.23 Hz, J = 8.16 Hz), 7.44 (1H, m, Ar-H), 7.65 (1H, dd, Ar-H, J = 1.17 Hz, J = 8.05 Hz), 7.78 (1H, s, 1,3-thiazole ring C-5), 7.87 (1H, dd, Ar-H, J = 1.69 Hz, J = 7.91 Hz), 8.30 (1H, s, –CH=N– azomethine), 12.50 (1H, s, –N–NH–C–); ^{13}C-NMR (75 MHz): δ 14.6 (–CH_3 ester), 60.9 (–OCH_2– ester), 119.8 (1,3-thiazole ring C-5), 123.1, 127.1, 128.6, 131.5, 133.3, 133.6 (Ar-C), 140.4 (–CH=N– azomethine), 143.3 (1,3-thiazole ring C-4), 161.4 (C=O), 168.3 (1,3-thiazole ring C-2); HRMS (MALDI-TOF): calcd $C_{13}H_{12}BrN_3NaO_2S$ (M + Na) = 375.97313, found: 376.12838.

Ethyl 2-(2-(1-phenylethylidene)hydrazinyl)thiazole-4-carboxylate (1g). Dark yellow solid; yield: 61%; melting point: 108–110 °C; R_f: 0.60 (acetone/*n*-hexane, 1 : 2); IR (ATR, cm^{-1}): 1087 (C–O stretching, ester), 1442 (C–H bending, aliphatic), 1573 (C=C ring stretching), 1699 (C=N stretching), 1712 (C=O stretching), 2978 (C–H stretching, aliphatic); ^{1}H-NMR (500 MHz): δ 1.27 (3H, t, –CH_3 ester, J = 7.14 Hz), 2.29 (3H, s, –CH_3), 4.23 (2H, q, –CH_2–CH_3 ester, J = 7.08 Hz), 7.39 (3H, m, Ar-H), 7.75 (2H, m, Ar-H + 1,3-thiazole ring C-5), 7.91 (1H, s, –CH=N– azomethine), 12.31 (1H, s, –N–NH–C–); ^{13}C-NMR (126 MHz): δ 14.2 (–CH_3 ester), 14.9 (–CH_3), 60.8 (–OCH_2– ester), 119.7 (1,3-thiazole ring C-5), 126.2, 128.7, 128.9, 129.3 (Ar-C), 138.2 (–CH=N– azomethine), 147.4 (1,3-thiazole ring C-4), 161.6 (C=O), 170.1 (1,3-thiazole ring C-2); HRMS (MALDI-TOF): calcd $C_{14}H_{15}N_3NaO_2S$ (M + Na) = 312.0783, found: 311.86282.

Ethyl 2-(2-(furan-2-ylmethylene)hydrazinyl)thiazole-4-carboxylate (1h). Dark green solid; yield: 73%; melting point: 215–217 °C; R_f: 0.52 (acetone/*n*-hexane, 1 : 2); IR (ATR, cm^{-1}): 1091 (C–O stretching, ester), 1431 (C–H bending, aliphatic), 1573 (C=C ring stretching), 1622 (C=N stretching), 1720 (C=O stretching), 2976 (C–H stretching, aliphatic); ^{1}H-NMR (500 MHz): δ 1.26 (3H, t, –CH_3 ester, J = 7.12 Hz), 4.22 (2H, q, –CH_2–CH_3 ester, J = 7.05 Hz), 6.59 (1H, m, Ar-H), 6.81 (1H, d, Ar-H, J = 3.41 Hz), 7.73 (1H, s, 1,3-thiazole ring C-5), 7.78 (1H, m, Ar-H), 7.86 (1H, s, –CH=N– azomethine), 12.54 (1H, s, –N–NH–C–); ^{13}C-NMR (126 MHz): δ 14.6 (–CH_3 ester), 60.8 (–OCH_2– ester), 119.7 (1,3-thiazole ring C-5), 112.5, 113.1, 145.1, 149.5 (Ar-C), 132.6 (–CH=N– azomethine), 143.2 (1,3-thiazole ring C-4), 161.4 (C=O), 168.3 (1,3-thiazole ring C-2); HRMS (MALDI-TOF): calcd $C_{11}H_{11}N_3NaO_3S$ (M + Na) = 288.0419, found: 287.63438.

Synthesis of alkyl 2-(2-(arylidene)hydrazono)-4-oxothiazolidine-5-acetates (2a–p)

Thionyl chloride (2.0 equivalent) and the respective alcohol (20 mL) were initially stirred together at 0 °C, followed by the addition of 2-(2-(arylidene)hydrazono)-4-oxothiazolidine-5-acetic acids (1.0 mmol). The reaction mixture was further

stirred at room temperature for 30 to 50 minutes. The reaction mixture was then refluxed for 30 to 50 minutes. Conversion of acids into respective esters was observed by taking TLC (acetone : *n*-hexane; 1 : 3). The solid appeared when the reaction mixture was put on ice, which was filtered and washed with an excess of water. The esters were dried at room temperature.

Ethyl 2-((2-benzylidene)hydrazono)-4-oxothiazolidine-5-acetate (2a). White solid; yield: 96%; melting point: 224–226 °C; R_f: 0.33 (acetone/*n*-hexane, 1 : 3); IR (ATR, cm^{-1}): 1018 (C–O stretching, ester), 1338 (C–H bending, aliphatic), 1516 (C=C ring stretching), 1643 (C=N stretching), 1708 (C=O stretching), 2993 (C–H stretching, aliphatic); ^{1}H-NMR (300 MHz): δ 1.19 (3H, t, –CH_3, ester, J = 7.05 Hz), 2.68 (1H, dd, –CH_2–, J = 9.70 Hz, J = 16.95 Hz), 3.08 (1H, dd, –CH_2-, J = 3.75 Hz, J = 16.95 Hz), 4.10 (2H, q, –CH_2–CH_3 ester, J = 6.45 Hz), 4.50 (1H, dd, 1,3-thiazolidin-4-one ring C-5, J = 4.50 Hz, J = 7.70 Hz), 7.42 (3H, m, Ar-H), 7.70 (2H, m, Ar-H), 8.29 (1H, s, –CH=N– azomethine); ^{13}C-NMR (75 MHz): δ 14.5 (–CH_3 ester), 38.6 (–CH_2–), 45.8 (1,3-thiazolidin-4-one ring C-5), 60.9 (–OCH_2– ester), 127.5, 127.8, 129.2, 130.1 (Ar-C), 135.7 (–CH=N– azomethine), 152.6 (1,3-thiazolidin-4-one ring C-2), 171.5 (C=O), 181.9 (1,3-thiazolidin-4-one ring C-4); HRMS (MALDI-TOF): calcd $C_{14}H_{15}N_3NaO_3S$ (M + Na) = 328.07318, found: 329.35526.

Methyl 2-(2-(4-chlorobenzylidene)hydrazono)-4-oxothiazolidine-5-acetate (2b). White solid; yield: 87%; melting point: 218–220 °C; R_f: 0.45 (acetone/*n*-hexane, 1 : 3); IR (ATR, cm^{-1}): 1087 (C–O stretching, ester), 1442 (C–H bending, aliphatic), 1600 (C=C ring stretching), 1643 (C=N stretching), 1712 (C=O stretching), 1735 (C=O stretching), 2985 (C–H stretching, aliphatic); ^{1}H-NMR (300 MHz): δ 3.01 (1H, dd, –CH_2–, J = 8.40 Hz, J = 17.70 Hz), 3.11 (1H, dd, –CH_2-, J = 4.30 Hz, J = 17.30 Hz), 3.64 (3H, s, –OCH_3), 4.42 (1H, dd, 1,3-thiazolidin-4-one ring C-5, J = 4.20 Hz, J = 8.30 Hz), 7.56 (2H, m, Ar-H), 7.77 (2H, d, Ar-H, J = 8.40 Hz), 8.41 (1H, s, –CH=N– azomethine), 12.08 (1H, s, –NH); ^{13}C-NMR (75 MHz): δ 36.6 (-CH_2-), 43.8 (1,3-thiazolidin-4-one ring C-5), 52.4 (–OCH_3), 129.4, 130.5, 133.1, 136.5 (Ar-C), 155.5 (–CH=N– azomethine), 165.3 (1,3-thiazolidin-4-one ring C-2), 171.3 (C=O), 175.8 (1,3-thiazolidin-4-one ring C-4); HRMS (MALDI-TOF): calcd $C_{12}H_{13}ClN_3NaO_3S$ (M + Na) = 348.0186, found: 348.04657.

Ethyl 2-(2-(2-chlorobenzylidene)hydrazono)-4-oxothiazolidine-5-acetate (2c). White solid; yield: 89%; melting point: 210–212 °C; R_f: 0.47 (acetone/*n*-hexane, 1 : 3); IR (ATR, cm^{-1}): 1086 (C–O stretching, ester), 1445 (C–H bending, aliphatic), 1601 (C=C ring stretching), 1647 (C=N stretching), 1710 (C=O stretching), 1731 (C=O stretching), 2985 (C–H stretching, aliphatic); ^{1}H-NMR (300 MHz): δ 1.17 (3H, t, –CH_3, ester, J = 7.03 Hz), 2.67 (1H, dd, –CH_2-, J = 9.69 Hz, J = 16.95 Hz), 3.08 (1H, dd, –CH_2–, J = 3.70 Hz, J = 16.95 Hz), 4.08 (2H, q, –CH_2–CH_3 ester, J = 6.45 Hz), 4.42 (1H, dd, 1,3-thiazolidin-4-one ring C-5, J = 4.20 Hz, J = 8.30 Hz), 7.56 (2H, m, Ar-H), 7.77 (2H, d, Ar-H, J = 8.40 Hz), 8.41 (1H, s, –CH=N– azomethine), 12.02 (1H, s, –NH); ^{13}C-NMR (75 MHz): δ 14.5 (–CH_3 ester), 38.7 (–CH_2–), 45.7 (1,3-thiazolidin-4-one ring C-5), 60.8 (–OCH_2– ester), 127.5, 127.8, 131.2, 132.1 (Ar-C), 136.7 (-CH=N- azomethine), 153.6 (1,3-thiazolidin-4-one ring C-2), 173.5 (C=O), 181.9 (1,3-thiazolidin-4-one ring C-4); HRMS (MALDI-TOF): calcd $C_{14}H_{14}ClN_3NaO_3S$ (M + Na) = 362.03421, found: 362.12087.

Ethyl 2-(2-(4-bromobenzylidene)hydrazono)-4-oxothiazolidine-5-acetate (2d). White solid; yield: 90%; melting point: 208–210 °C; R_f: 0.41 (acetone/*n*-hexane, 1 : 3); IR (ATR, cm^{-1}): 1010 (C–O stretching, ester), 1334 (C–H bending, aliphatic), 1512 (C=C ring stretching), 1643 (C=N stretching), 1712 (C=O stretching), 2981 (C–H stretching, aliphatic); ^{1}H-NMR (300 MHz): δ 1.18 (3H, t, –CH_3, J = 6.90 Hz), 2.98 (1H, dd, –CH_2–, J = 7.80 Hz, J = 17.40 Hz), 3.08 (1H, dd, –CH_2–, J = 4.50 Hz, J = 17.85 Hz), 4.09 (2H, q, –CH_2–CH_3 ester, J = 6.60 Hz), 4.41 (1H, dd, 1,3-thiazolidin-4-one ring C-5, J = 4.50 Hz, J = 7.80 Hz), 7.69 (4H, m, Ar-H), 8.40 (1H, s, –CH=N– azomethine), 12.09 (1H, s, –NH); ^{13}C-NMR (75 MHz): δ 14.4 (–CH_3), 36.8 (–CH_2–), 43.8 (1,3-thiazolidin-4-one ring C-5), 61.1 (–OCH_2– ester), 124.5, 129.7, 129.9, 130.7, 132.1, 132.3 (Ar-C), 132.4 (–CH=N– azomethine), 133.9 (1,3-thiazolidin-4-one ring C-2), 155.7 (C=O), 170.6 (1,3-thiazolidin-4-one ring C-4); HRMS (MALDI-TOF): calcd $C_{14}H_{14}BrN_3NaO_3S$ (M + Na) = 405.98369, found: 406.43054.

Ethyl 2-(2-(3-bromobenzylidene)hydrazono)-4-oxothiazolidine-5-acetate (2e). White solid; yield: 91%; melting point: 218–220 °C; R_f: 0.43 (acetone/*n*-hexane, 1 : 3); IR (ATR, cm^{-1}): 1021 (C–O stretching, ester), 1341 (C–H bending, aliphatic), 1600 (C=C ring stretching), 1647 (C=N stretching), 1710 (C=O stretching), 2981 (C–H stretching, aliphatic); ^{1}H-NMR (300 MHz): δ 1.19 (3H, t, –CH_3, J = 6.89 Hz), 2.99 (1H, dd, –CH_2–, J = 7.80 Hz, J = 17.40 Hz), 3.08 (1H, dd, –CH_2–, J = 4.50 Hz, J = 17.85 Hz), 4.10 (2H, q, –CH_2–CH_3 ester, J = 6.65 Hz), 4.42 (1H, dd, 1,3-thiazolidin-4-one ring C-5, J = 4.52 Hz, J = 7.80 Hz), 7.78 (4H, m, Ar-H), 8.42 (1H, s, –CH=N– azomethine), 11.51 (1H, s, –NH); ^{13}C-NMR (75 MHz): δ 14.4 (–CH_3), 38.7 (–CH_2–), 43.9 (1,3-thiazolidin-4-one ring C-5), 61.2 (–OCH_2– ester), 124.5, 129.7, 129.9, 130.7, 132.1, 132.4 (Ar-C), 133.5 (–CH=N– azomethine), 135.9 (1,3-thiazolidin-4-one ring C-2), 159.7 (C=O), 172.6 (1,3-thiazolidin-4-one ring C-4); HRMS (MALDI-TOF): calcd $C_{14}H_{14}BrN_3NaO_3S$ (M + Na) = 405.98369, found: 406.89014.

Ethyl 2-(2-(4-nitrobenzylidene)hydrazono)-4-oxothiazolidine-5-acetate (2f). Yellow solid; yield: 80%; melting point: 226–228 °C; R_f: 0.29 (acetone/*n*-hexane, 1 : 3); IR (ATR, cm^{-1}): 1033 (C–O stretching, ester), 1342 (C–H bending, aliphatic), 1518 (C=C ring stretching), 1643 (C=N stretching), 1728 (C=O stretching), 2985 (C–H stretching, aliphatic); ^{1}H-NMR (300 MHz): δ 1.19 (3H, t, –CH_3, ester, J = 6.90 Hz), 2.97 (1H, dd, –CH_2–, J = 6.90 Hz, J = 16.95 Hz) 3.09 (1H, dd, –CH_2–, J = 3.30 Hz, J = 17.70 Hz), 4.10 (2H, q, –CH_2–CH_3 ester, J = 6.60 Hz), 4.40 (1H, dd, 1,3-thiazolidin-4-one ring C-5, J = 4.10 Hz, J = 7.70 Hz), 8.00 (2H, d, Ar-H, J = 7.80 Hz), 8.30 (2H, d, Ar-H, J = 8.10 Hz), 8.53 (1H, s, –CH=N– azomethine), 12.00 (1H, s, –NH); ^{13}C-NMR (75 MHz): δ 14.4 (–CH_3, ester), 37.0 (–CH_2–), 44.2 (1,3-thiazolidin-4-one ring C-5), 61.1 (–OCH_2– ester), 124.6, 128.9, 141.0, 148.5 (Ar-C), 154.0 (–CH=N– azomethine), 168.7 (1,3-thiazolidin-4-one ring C-2), 170.8 (C=O), 176.9 (1,3-thiazolidin-4-one ring C-4); HRMS (MALDI-TOF): calcd $C_{14}H_{14}N_4NaO_5S$ (M + Na) = 373.05826, found: 373.37363.

Ethyl 2-(2-(3-nitrobenzylidene)hydrazono)-4-oxothiazolidine-5-acetate (2g). White solid; yield: 88%; melting point: 191–193 °C; R_f: 0.27 (acetone/*n*-hexane, 1 : 3); IR (ATR, cm^{-1}): 1080 (C–O stretching, ester), 1354 (C–H bending, aliphatic), 1523 (C=C ring stretching), 1627 (C=N stretching), 1732 (C=O stretching), 3093 (C–H stretching, aliphatic); ^{1}H-NMR (300

MHz): δ 1.19 (3H, t, –CH_3 ester, J = 7.00 Hz), 3.03 (1H, dd, –CH_2-, J = 7.50 Hz, J = 17.40 Hz), 3.12 (1H, dd, –CH_2–, J = 4.80 Hz, J = 9.00 Hz), 4.10 (2H, q, –CH_2–CH_3 ester, J = 6.60 Hz), 4.45 (1H, dd, 1,3-thiazolidin-4-one ring C-5, J = 4.80 Hz, J = 7.50 Hz), 7.76 (1H, t, Ar-H, J = 8.00 Hz), 8.1 (1H, d, Ar-H, J = 7.80 Hz), 8.29 (1H, dd, Ar-H, J = 1.65 Hz, J = 8.25 Hz), 8.50 (1H, s, Ar-H), 8.58 (1H, s, –CH=N– azomethine), 12.17 (1H, s, –NH); ^{13}C-NMR (75 MHz): δ 14.4 (–CH_3 ester), 36.6 (–CH_2–), 43.9 (1,3-thiazolidin-4-one ring C-5), 61.1 (–OCH_2– ester), 122.3, 125.3, 130.9, 133.9, 136.4, 148.6 (Ar-C), 154.9 (–CH=N– azomethine), 166.3 (1,3-thiazolidin-4-one ring C-2), 170.7 (C=O), 175.8 (1,3-thiazolidin-4-one ring C-4); HRMS (MALDI-TOF): calcd $C_{14}H_{14}N_4NaO_5S$ (M + Na) = 373.05826, found: 373.27241.

Ethyl 2-(2-(2-nitrobenzylidene)hydrazono)-4-oxothiazolidine-5-acetate (2h). Off white solid; yield: 86%; melting point: 189–190 °C; R_f: 0.37 (acetone/*n*-hexane, 1 : 3); IR (ATR, cm^{-1}): 1086 (C–O stretching, ester), 1387 (C–H bending, aliphatic), 1589 (C=C ring stretching), 1643 (C=N stretching), 1730 (C=O stretching), 3089 (C–H stretching, aliphatic); ^{1}H-NMR (300 MHz): δ 1.19 (3H, t, –CH_3 ester, J = 7.01 Hz), 3.09 (1H, dd, –CH_2-, J = 7.55 Hz, J = 17.45 Hz), 3.13 (1H, dd, –CH_2–, J = 4.90 Hz, J = 9.00 Hz), 4.12 (2H, q, –CH_2–CH_3 ester, J = 6.65 Hz), 4.42 (1H, dd, 1,3-thiazolidin-4-one ring C-5, J = 4.85 Hz, J = 7.55 Hz), 7.78 (4H, m, Ar-H), 8.60 (1H, s, –CH=N– azomethine); ^{13}C-NMR (75 MHz): δ 14.4 (–CH_3 ester), 36.8 (–CH_2–), 42.9 (1,3-thiazolidin-4-one ring C-5), 61.2 (–OCH_2– ester), 123.4, 126.3, 131.9, 133.9, 136.5, 149.6 (Ar-C), 155.9 (–CH=N– azomethine), 165.3 (1,3-thiazolidin-4-one ring C-2), 171.7 (C=O), 176.9 (1,3-thiazolidin-4-one ring C-4); HRMS (MALDI-TOF): calcd $C_{14}H_{14}N_4NaO_5S$ (M + Na) = 373.05826, found: 373.27236.

Ethyl 2-(2-(4-methoxybenzylidene)hydrazono)-4-oxothiazolidine-5-acetate (2i). White solid; yield: 94%; melting point: 201–203 °C; R_f: 0.36 (acetone/*n*-hexane, 1 : 3); IR (ATR, cm^{-1}): 1033 (C–O stretching, ester), 1311 (C–H bending, aliphatic), 1512 (C=C ring stretching), 1651 (C=N stretching), 1720 (C=O stretching), 2989 (C–H stretching, aliphatic); ^{1}H-NMR (300 MHz): δ 1.18 (3H, t, –CH_3 ester, J = 7.20 Hz), 2.97 (1H, dd, –CH_2–, J = 8.10 Hz, J = 17.40 Hz), 3.07 (1H, dd, –CH_2-, J = 4.35 Hz, J = 17.55 Hz), 3.81 (3H, s, –OCH_3), 4.09 (2H, q, –CH_2–CH_3 ester, J = 6.30 Hz), 4.38 (1H, dd, 1,3-thiazolidin-4-one ring C-5, J = 4.50 Hz, J = 7.80 Hz), 7.03 (2H, d, Ar-H, J = 9.00 Hz), 7.69 (2H, d, Ar-H, J = 8.70 Hz), 8.33 (1H, s, –CH=N– azomethine), 12.03 (1H, s, –NH); ^{13}C-NMR (75 MHz): δ 14.4 (–CH_3 ester), 36.9 (–CH_2–), 43.8 (1,3-thiazolidin-4-one ring C-5), 55.8 (–OCH_3), 61.1 (–OCH_2– ester), 114.8, 127.3, 129.9, 161.7 (Ar-C), 156.2 (-CH=N- azomethine), 170.7 (1,3-thiazolidin-4-one ring C-2), 175.9 (C=O), 189.2 (1,3-thiazolidin-4-one ring C-4); HRMS (MALDI-TOF): calcd $C_{15}H_{17}N_3NaO_4S$ (M + Na) = 358.08375, found: 359.64858.

Ethyl 2-(2-(2-methoxybenzylidene)hydrazono)-4-oxothiazolidine-5-acetate (2j). White solid; yield: 96%; melting point: 189–191 °C; R_f: 0.39 (acetone/*n*-hexane, 1 : 3); IR (ATR, cm^{-1}): 1018 (C–O stretching, ester), 1334 (C–H bending, aliphatic), 1521 (C=C ring stretching), 1639 (C=N stretching), 1720 (C=O stretching), 2985 (C–H stretching, aliphatic); ^{1}H-NMR (300 MHz): δ 1.18 (3H, t, –CH_3, ester, J = 7.20 Hz), 2.97 (1H, dd, –CH_2–, J = 8.10 Hz, J = 17.40 Hz), 3.07 (1H, dd, –CH_2–, J = 4.50 Hz, J = 17.40 Hz), 3.88 (3H, s, –OCH_3), 4.03 (2H, q, –CH_2–CH_3 ester, J = 6.00 Hz), 4.38 (1H, dd, 1,3-thiazolidin-4-one ring C-5, J = 4.50 Hz, J = 7.80 Hz), 7.01 (1H, t, Ar, J = 7.50 Hz), 7.10 (1H, d, Ar, J = 8.40 Hz), 7.45 (1H, t, Ar-H, J = 8.40 Hz), 7.82 (1H, d, Ar-H, J = 7.80 Hz), 8.60 (1H, s, –CH=N– azomethine), 12.07 (1H, s, –NH); ^{13}C-NMR (75 MHz): δ 14.5 (-CH_3, ester), 36.9 (–CH_2–), 43.9 (1,3-thiazolidin-4-one ring C-5), 56.2 (–OCH_3), 61.1 (–OCH_2– ester), 112.4, 121.2, 122.5, 126.5, 132.7, 151.5 (Ar-C), 158.5 (–CH=N– azomethine), 170.7 (1,3-thiazolidin-4-one ring C-2), 176.2 (C=O), 189.2 (1,3-thiazolidin-4-one ring C-4); HRMS (MALDI-TOF): calcd $C_{15}H_{17}N_3NaO_4S$ (M + Na) = 358.08375, found: 358.19232.

Ethyl 2-(2-(3-hydroxybenzylidene)hydrazono)-4-oxothiazolidine-5-acetate (2k). Off white solid; yield: 80%; melting point: 236–238 °C; R_f: 0.26 (acetone/*n*-hexane, 1 : 3); IR (ATR, cm^{-1}): 1022 (C–O stretching, ester), 1330 (C–H bending, aliphatic), 1600 (C=C ring stretching), 1647 (C=N stretching), 1732 (C=O stretching), 2993 (C–H stretching, aliphatic); ^{1}H-NMR (300 MHz): δ 1.18 (3H, t, –CH_3 ester, J = 7.05 Hz), 2.99 (1H, dd, –CH_2-, J = 8.10 Hz, J = 17.70 Hz), 3.08 (1H, dd, –CH_2–, J = 4.50 Hz, J = 17.70 Hz), 4.17 (2H, q, –CH_2–CH_3 ester, J = 6.90 Hz), 4.40 (1H, dd, 1,3-thiazolidin-4-one ring C-5, J = 4.50 Hz, J = 7.80 Hz), 6.87 (1H, m, Ar-H), 7.19 (3H, m, Ar-H), 8.30 (1H, s, –CH=N– azomethine), 9.74 (1H, s, –OH), 12.04 (1H, s, –NH); ^{13}C-NMR (75 MHz): δ 14.5 (–CH_3 ester), 36.9 (–CH_2–), 43.8 (1,3-thiazolidin-4-one ring C-5), 61.1 (–OCH_2– ester), 113.7, 118.5, 119.8, 130.3, 135.8, 158.1 (Ar-C), 156.9 (–CH=N– azomethine), 170.7 (1,3-thiazolidin-4-one ring C-2), 175.8 (C=O), 189.2 (1,3-thiazolidin-4-one ring C-4); HRMS (MALDI-TOF): calcd $C_{14}H_{15}N_3NaO_4S$ (M + Na) = 344.0681, found: 344.16745.

Ethyl 2-(2-(2-hydroxybenzylidene)hydrazono)-4-oxothiazolidine-5-acetate (2l). Light green solid; yield: 91%; melting point: 248–250 °C; R_f: 0.33 (acetone/*n*-hexane, 1 : 3); IR (ATR, cm^{-1}): 1014 (C–O stretching, ester), 1338 (C–H bending, aliphatic), 1525 (C=C ring stretching), 1639 (C=N stretching), 1716 (C=O stretching), 2989 (C–H stretching, aliphatic); ^{1}H-NMR (300 MHz): δ 1.18 (3H, t, –CH_3 ester, J = 6.75 Hz), 3.03 (1H, dd, –CH_2–, J = 8.10 Hz, J = 17.40 Hz), 3.09 (1H, dd, –CH_2-, J = 4.20 Hz, J = 7.10 Hz), 4.10 (2H, q, –CH_2–CH_3 ester, J = 6.45 Hz), 4.50 (1H, dd, 1,3-thiazolidin-4-one ring C-5, J = 4.20 Hz, J = 6.30 Hz), 6.95 (2H, m, Ar-H), 7.35 (1H, m, Ar-H), 7.65 (1H, m, Ar-H), 8.64 (1H, s, –CH=N– azomethine), 10.87 (1H, s, –OH), 12.16 (1H, s, –NH); ^{13}C-NMR (75 MHz): δ 14.4 (-CH_3, ester), 36.6 (–CH_2–), 44.2 (1,3-thiazolidin-4-one ring C-5), 61.2 (–OCH_2– ester), 116.8, 118.9, 119.9, 130.8, 132.7, 159.1 (Ar-C), 158.5 (–CH=N– azomethine), 170.6 (1,3-thiazolidin-4-one ring C-2), 175.5 (C=O), 189.2 (1,3-thiazolidin-4-one ring C-4); HRMS (MALDI-TOF): calcd $C_{14}H_{15}N_3NaO_4S$ (M + Na) = 344.0681, found: 344.11239.

Ethyl 2-(2-(4-methylbenzylidene)hydrazono)-4-oxothiazolidine-5-acetate (2m). Light yellow solid; yield: 77%; melting point: 253–255 °C; R_f: 0.33 (acetone/*n*-hexane, 1 : 3); IR (ATR, cm^{-1}): 1014 (C–O stretching, ester), 1336 (C–H bending, aliphatic), 1618 (C=C ring stretching), 1647 (C=N stretching), 1712, 1726 (C=O stretching), 2987 (C–H stretching, aliphatic); ^{1}H-NMR (300 MHz): δ 1.19 (3H, t, –CH_3 ester, J = 7.00 Hz), 2.34 (3H, s, –CH_3), 2.99 (1H, dd, –CH_2–, J = 8.10 Hz, J = 17.70 Hz), 3.08 (1H, dd, –CH_2-, J = 4.50 Hz, J = 17.40 Hz), 4.10 (2H, q, –CH_2–CH_3 ester, J = 6.30 Hz), 4.41 (1H, dd, 1,3-thiazolidin-4-one

ring C-5, $J = 4.50$ Hz, $J = 7.50$ Hz), 7.27 (2H, d, Ar-H, $J = 8.10$ Hz), 7.65 (2H, d, Ar-H, $J = 8.10$ Hz), 8.36 (1H, s, –CH=N– azomethine), 12.07 (1H, s, –NH); ^{13}C-NMR (75 MHz): δ 14.5 (–CH_3 ester), 21.6 (–CH_3), 36.8 (–CH_2–), 43.7 (1,3-thiazolidin-4-one ring C-5), 61.1 (–OCH_2–, ester), 128.1, 129.9, 131.9, 141.1 (Ar-C), 156.7 (–CH=N– azomethine), 163.9 (1,3-thiazolidin-4-one ring C-2), 170.7 (C=O), 175.8 (1,3-thiazolidin-4-one ring C-4); HRMS (MALDI-TOF): calcd $C_{15}H_{18}N_3NaO_3S$ (M + Na) = 342.08883, found: 342.11165.

Ethyl 2-(2-(2-methylbenzylidene)hydrazono)-4-oxothiazolidine-5-acetate (2n). White solid; yield: 93%; melting point: 226–228 °C; R_f: 0.28 (acetone/*n*-hexane, 1 : 3); IR (ATR, cm^{-1}): 1022 (C–O stretching, ester), 1338 (C–H bending, aliphatic), 1523 (C=C ring stretching), 1643 (C=N stretching), 1724 (C=O stretching), 2993 (C–H stretching, aliphatic); ^{1}H-NMR (300 MHz): δ 1.18 (3H, t, –CH_3, ester, $J = 7.20$ Hz), 2.49 (3H, s, –CH_3), 2.98 (1H, dd, –CH_2–, $J = 7.95$ Hz, $J = 17.55$ Hz), 4.09 (2H, q, –CH_2–CH_3 ester, $J = 7.20$ Hz), 4.39 (1H, dd, 1,3-thiazolidin-4-one ring C-5, $J = 4.50$ Hz, $J = 8.10$ Hz), 7.31 (3H, m, Ar-H), 7.76 (1H, m, Ar-H), 8.92 (1H, s, –CH=N– azomethine), 12.09 (1H, s, –NH); ^{13}C-NMR (75 MHz): δ 14.5 (–CH_3, ester), 20.4 (–CH_3), 36.9 (–CH_2-), 43.9 (1,3-thiazolidin-4-one ring C-5), 61.1 (–OCH_2–, ester), 126.6, 128.4, 130.6, 131.6, 132.6, 137.9 (Ar-C), 155.8 (–CH=N– azomethine), 170.7 (1,3-thiazolidin-4-one ring C-2), 176.3 (C=O), 189.2 (1,3-thiazolidin-4-one ring C-4); HRMS (MALDI-TOF): calcd $C_{15}H_{18}N_3NaO_3S$ (M + Na) = 342.08883, found: 342.07265.

Ethyl 2-((2-(3,4-dihydronaphthalen-1(2*H*)-ylidene)) hydrazono)-4-oxo-thiazolidin-5-acetate (2o). Brown solid; yield: 69%; melting point: 246–248 °C; R_f: 0.30 (acetone/*n*-hexane, 1 : 3); IR (ATR, cm^{-1}): 1031 (C–O stretching, ester), 1346 (C–H bending, aliphatic), 1616 (C=C ring stretching), 1716 (C=O stretching), 2909 (C–H stretching, aliphatic); ^{1}H-NMR (300 MHz): δ 1.18 (3H, t, –CH_3 ester, $J = 7.20$ Hz), 1.81 (2H, m, –CH_2–, tetralone), 2.79 (4H, m, tetralone), 2.98 (1H, dd, –CH_2–, $J = 7.80$ Hz, $J = 17.40$ Hz), 3.07 (1H, dd, –CH_2–, $J = 4.50$ Hz, $J = 17.40$ Hz), 4.09 (2H, q, –CH_2–CH_3 ester, $J = 6.90$ Hz), 4.37 (1H, dd, 1,3-thiazolidin-4-one ring C-5, $J = 4.50$ Hz, $J = 7.80$ Hz), 7.26 (3H, m, tetralone), 8.06 (1H, m, tetralone), 12.01 (1H, s, –NH); ^{13}C-NMR (75 MHz): δ 14.6 (–CH_3 ester), 22.3, 27.4, 29.6 (3-CH_2–, tetralone), 36.9 (–CH_2–), 43.4 (1,3-thiazolidin-4-one ring C-5), 61.1 (–OCH_2–, ester), 125.0, 126.6, 129.3, 130.2, 132.6, 140.9 (Ar-C), 160.3 (–C=N–), 162.9 (1,3-thiazolidin-4-one ring C-2), 170.7 (C=O), 175.6 (1,3-thiazolidin-4-one ring C-4); HRMS (MALDI-TOF): calcd $C_{17}H_{19}N_3NaO_5S$ (M + Na) = 368.01448, found: 368.27513.

Ethyl 2-(2-(4-hydroxy-3-methoxybenzylidene)hydrazono)-4-oxothiazolidine-5-acetate (2p). Off white solid; yield: 91%; melting point: 226–228 °C; R_f: 0.30 (acetone/*n*-hexane, 1 : 3); IR (ATR, cm^{-1}): 1026 (C–O stretching, ester), 1338 (C–H bending, aliphatic), 1595 (C=C ring stretching), 1637 (C=N stretching), 1724 (C=O stretching), 2990 (C–H stretching, aliphatic), 3375 (–OH, stretching); ^{1}H-NMR (300 MHz): δ 1.18 (3H, t, –CH_3, ester, $J = 7.20$ Hz), 3.04 (1H, dd, –CH_2–, $J = 4.80$ Hz, $J = 13.20$ Hz), 3.01 (1H, dd, –CH_2–, $J = 4.80$ Hz, $J = 13.20$ Hz), 3.80 (3H, s, –OCH_3), 4.09 (2H, q, –CH_2–CH_3 ester, $J = 7.20$ Hz), 4.38 (1H, dd, 1,3-thiazolidin-4-one ring C-5, $J = 4.50$ Hz, $J = 7.50$ Hz), 6.84 (1H, d, Ar-H, $J = 8.10$ Hz), 7.18 (1H, dd, Ar-H, $J = 1.50$ Hz, $J = 8.40$ Hz), 7.31 (1H, d, Ar-H, $J = 1.50$ Hz), 8.26 (1H, s, –CH=N– azomethine), 9.65 (1H, s, –OH), 11.94 (1H, s, –NH); ^{13}C-NMR (75 MHz): δ solubility issue. HRMS (MALDI-TOF): calcd $C_{15}H_{17}N_3NaO_5S$ (M + Na) = 374.07866, found: 374.31122.

In vitro evaluation and mechanism of action assays

Cell assays. The trypomastigote forms of *T. cruzi* (Y strain) were maintained in DMEM (Dulbecco's Modified Eagle Medium) medium, pH 7.2 supplemented with 10% SFB and incubated at 37 °C with 5% CO_2. LLC-MK2 cells (Monkey kidney epithelial cells [*Macaca mulatta*]; CCL-7; American Type Culture Collection, Rockville, MD, USA) were cultured in DMEM medium, pH 7.2, supplemented with 10% L-glutamine SFB, and incubated at 37 °C in a 5% CO_2 atmosphere. *L. amazonensis* and *L. infantum* (WHOM/00LTB0016 and MHOM/MA/67/ITMAP-263, respectively) promastigote forms were maintained in Schneider's insect medium, pH 7.2 supplemented with 10% SFB and incubated at 26 °C.

Cytotoxicity on mammalian cells. Cytotoxicity was evaluated in LLC-MK2 cells using the MTT reduction cell viability assay (MOSSMANN, 1983). This method is based on the ability of mitochondrial dehydrogenase enzymes to convert the water-soluble tretazolium (3-[4,5-dimethylthiazol-2-yl]-2,5-diphenyltetra-zolium bromide) salt to an insoluble purple substance called Formazan.

For this purpose, LLC-MK2 cells (2.5×10^5 cells per mL) in DMEM medium supplemented with 10% SFB were cultured in 96-well plates, and maintained at 37 °C and 5% CO_2 for 24 h. The substances were then added at increasing concentrations (10, 50, 100, 500, and 1000 μM), and the plate incubated for 96 hours. After treatment, cells were washed with PBS (pH 7.2) and incubated in the presence of MTT (2 mg mL^{-1}) for 4 hours. The supernatant was removed, the Formazan crystals were solubilized in DMSO, and the absorbance reading was taken at 570 nm on a plate spectrophotometer (Power Wave XS-BioTek). The percentage of viable cells was calculated concerning the control. The CC_{50} values (50% cytotoxic concentration) were determined by nonlinear regression analysis.

Amastigote assay. For the amastigote assay, *T. cruzi* amastigote forms of Tulahuen strain expressing the *Escherichia coli* beta-galactosidase gene were grown on a monolayer of mouse L-929 fibroblasts. Cultures assayed for beta-galactosidase activity were grown in RPMI 1640 medium without phenol red plus 10% fetal bovine serum and glutamine. Ninety-six-well tissue culture microplates were seeded with L-929 fibroblasts at 4.0×10^3 per well in 80 μL, and incubated overnight at 37 °C, 5% CO_2. Beta-galactosidase-expressing trypomastigotes were then added at 4.0×10^4 per well in 20 μL. After 2 hours, the medium with trypomastigotes that have not penetrated the cells was discarded, and replaced by 200 μL of fresh medium. After 48 hours, the medium was discarded again, and replaced by 180 μL of fresh medium and 20 μL of test compounds dissolved in DMSO. Each compound was tested in quadruplicate. After 7 days of culture development, chlorophenol red beta-D-galactopyranoside at 100 μM and Nonidet P-40 at 0.1% were added to the

plates, and incubated overnight at 37 °C. The absorbance was measured at 570 nm in an automated microplate reader. **BZD** at 3.81 μM (IC_{50}) was used as a positive control. The results are expressed as a percentage of parasite growth inhibition. Two independent experiments were performed.

Trypomastigote assay. Trypomastigote forms (1×10^7 parasites per mL) in DMEM medium supplemented with 10% SFB were added to 96-well microplates in the presence and absence of increasing concentrations (1, 5, 10, 50, 100 μM) of the substances, and incubated for 24 hours at 37 °C in a 5% CO_2 atmosphere. The result was obtained by observing the mortality, allowing the determination of parasite viability using the Brener method (BRENER, 1962). It consists of the parasite count of 50 fields of 5 μL of the slide-cover slip sample, and the EC_{50} (effective concentration for 50% of the parasites) was finally calculated by nonlinear regression.

Ultrastructural analysis. The samples of *T. cruzi* trypomastigote were cultured for 24 hours in RPMI 1640 medium (Sigma-Aldrich, St. Louis, MO, USA); buffered to pH 7.5 and supplemented with HEPES (20 mM), 10% fetal bovine serum, penicillin (100 U mL^{-1}) and streptomycin (100 mg mL^{-1}), containing the compound at the IC_{50} concentration (0.8 μM), twice (1.66 μM) and four times (3.32 μM) the value of IC_{50}. The parasites were collected, washed in PBS and fixed with 2.5% glutaraldehyde, 4% formaldehyde and 0.1 M cacodylate buffer at pH 6.8. They were then post fixed in 2% osmium tetroxide (OsO_4) in a 0.1 M cacodylate buffer at pH 6.8, and processed for routine scanning electron microscopy. The parasites were dehydrated in graded ethanol, and dried by the critical point method with CO_2. The samples were mounted on aluminum stubs, coated with gold, and examined under a JEOL-5600LV microscope (NPT/FIOCRUZ-PE). The controls were composed of untreated cells (negative control) and those treated with **BZD** (positive control).

***L. amazonensis* and *L. infantum* assay.** Promastigotes were incubated (1×10^6 cells per mL, Schneider's medium with 10% Fetal Bovine Serum) in a 96-well microplate with compounds in eight different concentrations (1.5 to 200 μg mL^{-1}) for 72 hours at 26 °C. Cells without treatment were used as negative controls, and Miltefosine was used as the standard. Cell growth was assessed and IC_{50}/72 hours was determined by regression analyses. Assays were conducted in triplicate.

Cell death assessment through flow cytometry

After confirmation of trypanocidal activity, Annexin-FITC/propidium iodide labeling was used to characterize cell death modalities induced by incubation with compounds. Metacyclic trypomastigotes were collected from the supernatant of infected L929 cells, and then seeded at 4×10^5 cells per well in RPMI-1640 medium. Compound **1f** was dissolved in DMSO, and added to wells at IC_{50}, $2 \times IC_{50}$, and $4 \times IC_{50}$ concentrations. Benznidazole (IC_{50}, $2 \times IC_{50}$, and $4 \times IC_{50}$) and the culture medium were used as a positive and negative control, respectively. Plates were incubated at the same conditions used for anti-trypomastigote activity (37 °C, 24 hours). Briefly, after treatment, parasites were washed with PBS and resuspended in binding buffer (Annexin V Binding Buffer- BD Pharmingen™, USA). For labeling, 10 μL of propidium iodide (50 μg mL^{-1}) and 5 μL of Annexin-FITC (BD Pharmingen™, USA) were added for 15 min at room temperature in the dark. Flow cytometry was conducted in a FACS Caliber (Becton & Dickinson, USA). For each sample, we acquired 20 000 events and the data were analyzed using Cell Quest software (Becton & Dickinson, USA). Assays were conducted in triplicate. For significance analysis, ANOVA and Dunnett's test was used, taking into account $p < 0.05$.

Conclusions

Eleven 1,3-thiazole-4-carboxylates and sixteen 4-thiazolidinone-acetates were obtained with reasonable yields using a simple methodology by bioisosteric and esterification strategies. These molecules were evaluated for their trypanocidal, leishmanicidal and cytotoxicity. Some of them exhibited very good trypanocidal activity, especially compounds **1f**, **1h**, **1g**, **1a**, and **2d**. From the tested scaffolds, the 1,3-thiazoles exhibited better trypanocidal activity than 4-thiazolidinones. The flow cytometry study showed that compound **1f** ($IC_{50} = 0.83$ μM) kills the parasite *via* necrosis and apoptosis. However, the activity was not observed in the amastigote form. Scanning electron microscopy analysis showed that compound **1f** at IC_{50} concentrations promoted alterations in the shape, flagella and surface of the body, inducing parasite death. Besides, compounds **1b**, **1f**, **2d** and **2m** exhibited better IC_{50} values for both *L. amazonensis* and *L. infantum* in comparison to standard Miltefosine. Our work corroborated the bioisosteric and esterification approaches for drug optimization and discovery with regards to chagas disease and leishmaniasis through 1,3-thiazole and 4-thiazolidinone scaffolds.

Conflicts of interest

The authors declare no conflict of interest.

Acknowledgements

Ana Cristina Lima Leite is receiving a CNPq senior fellowship. The authors are thankful for the Centro de Tecnologias Estratégicas do Nordeste (CETENE) for recording LCMS of all compounds. All authors declare no competing financial interest. The author Muhammad Haroon is grateful to Prof. Dr Alan S. Goldman. Department of chemistry and chemical biology, Rutgurs University New Brunswick 610 Taylor Road, Piscataway, NJ 08854-8087 USA for providing NMR facility. The corresponding author is thankful to Prof. Dr Shahid Hameed, Department of Chemistry, QAU, Islamabad-45320, Pakistan for providing NMR facility.

References

1 Laboratory of immunomodulation, Department of Protozoology/IOC – FIOCRUZ, *The Leishmaniasis*, 1997,

accessed on 28th August 2019, http://www.dbbm.fiocruz.br/tropical/leishman/leishext/html/morfologia.html.
2 Pan American Health Organization, *Leishmaniasis: Epidemiological Report in the Americas*, Pan American Health Organization, Washington, 2019, http://www.paho.org/leishmaniasis.
3 J. A. Urbina, *J. Eukaryotic Microbiol.*, 2015, **62**, 149–156.
4 M. J. Pinazo, L. Guerrero, E. Posada, E. Rodríguez, D. Soy and J. Gascon, *Antimicrob. Agents Chemother.*, 2013, **57**, 390e395.
5 D. H. Molyneux, L. Savioli and D. Engels, *Lancet*, 2017, **389**, 312–325.
6 J. A. Urbina and R. Docampo, *Trends Parasitol.*, 2003, **19**, 495–501.
7 J. Urbina, Chemotherapy of chagas disease, *Curr. Pharm. Des.*, 2002, **8**, 287–295.
8 A. L. Ribeiro, M. P. Nunes, M. M. Teixeira and M. O. C. Rocha, *Nat. Rev. Cardiol.*, 2012, **9**, 576–589.
9 C. Marín, I. Ramírez-Macías, M. J. Rosales, B. Muro, F. Reviriego, P. Navarro, V. J. Arán and M. Sánchez-Moreno, *Acta Trop.*, 2015, **148**, 170–178.
10 S. Espuelas, D. Plano, P. Nguewa, M. Font, J. A. Palop, J. M. Irache and C. Sanmartín, *Curr. Med. Chem.*, 2012, **19**, 4259–4288.
11 World Health Organization, *Defeating Neglected Tropical Diseases: Progress, Challenges and Opportunities*, WHO/CDS/NTD/2019.01, 2019, access in 8th September 2019, https://apps.who.int/iris/handle/10665/325755.
12 R. W. DeSimone, K. S. Currie, S. A. Mitchell, J. W. Darrow and D. A. Pippin, *Comb. Chem. High Throughput Screening*, 2004, **7**(5), 473–494.
13 J. Polanski, A. Kurczyk, A. Bak and R. Musiol, *Curr. Med. Chem.*, 2012, **19**(13), 1921–1945.
14 D. González Cabrera, F. Douelle, T.-S. Feng, A. T. Nchinda, Y. Younis, K. L. White, Q. Wu, E. Ryan, J. N. Burrows, D. Waterson, M. J. Witty, S. Wittlin, S. A. Charman and K. J. Chibale, *Med. Chem.*, 2011, **54**(21), 7713–7719.
15 P. A. de Moraes Gomes, M. de Oliveira Barbosa, E. Farias Santiago, M. V. de Oliveira Cardoso, N. T. Capistrano Costa, M. Z. Hernandes, D. R. Moreira, A. C. da Silva, T. A. Dos Santos, V. R. Pereira, F. A. Brayner Dos Santos, G. A. do Nascimento Pereira, R. S. Ferreira and A. C. Leite, *Eur. J. Med. Chem.*, 2016, **121**, 387–398.
16 G. C. Moraski, N. Seeger, P. A. Miller, A. G. Oliver, H. I. Boshoff, S. Cho, S. Mulugeta, J. R. Anderson, S. G. Franzblau and M. J. Mille, *ACS Infect. Dis.*, 2016, **2**, 393–398.
17 M. V. Cardoso, L. R. de Siqueira, E. B. da Silva, L. B. Costa, M. Z. Hernandes, M. M. Rabello, R. S. Ferreira, L. F. da Cruz, D. R. Moreira, V. R. Pereira, M. C. de Castro, P. V. Bernhardt and A. C. Leite, *Eur. J. Med. Chem.*, 2014, **86**, 48–59.
18 H. M. Ashour, I. M. El-Ashmawy and A. E. Bayad, *Monatsh. Chem.*, 2016, **147**, 605–618.
19 G. Cihan-Üstündağ, E. Gürsoy, L. Naesens, N. Ulusoy Güzeldemirci and G. Çapan, *Bioorg. Med. Chem.*, 2016, **24**(2), 240–246.
20 D. Secci, S. Carradori, B. Bizzarri, P. Chimenti, C. De Monte, A. Mollica, D. Rivanera, A. Zicari, E. Mari, G. Zengin and A. Aktumsek, *Eur. J. Med. Chem.*, 2016, **117**, 144–156.
21 D. R. Moreira, A. C. Leite, M. V. Cardoso, R. M. Srivastava, M. Z. Hernandes, M. M. Rabello, L. F. da Cruz, R. S. Ferreira, d. C. A. Simone, C. S. Meira, E. T. Guimaraes, A. C. da Silva, T. A. dos Santos, V. R. Pereira and M. B. Soares, *ChemMedChem*, 2014, **9**(1), 177–188.
22 G. B. de Oliveira Filho, M. V. de Oliveira Cardoso, J. W. Espíndola, L. F. Ferreira, C. A. de Simone, R. S. Ferreira, P. L. Coelho, C. S. Meira, M. D. R. Moreira, M. B. Soares and A. C. Lima Leite, *Bioorg. Med. Chem.*, 2015, **23**(23), 7478–7486.
23 G. B. de Oliveira Filho, M. V. d. O. Cardoso, J. W. P. Espíndola, D. A. Oliveira e Silva, R. S. Ferreira, P. L. Coelho, P. S. dos Anjos, E. d. S. Santos, C. S. Meira, D. R. M. Moreira, M. B. P. Soares and A. C. L. Leite, *Eur. J. Med. Chem.*, 2017, **141**, 346–361.
24 M. V. O. Cardoso, G. B. Oliveira Filho, L. R. P. Siqueira, J. W. P. Espíndola, E. B. D. Silva, A. P. O. Mendes, V. R. A. Pereira, M. C. A. B. Castro, R. S. Ferreira, F. S. Villela, F. M. R. D. Costa, C. S. Meira, D. R. M. Moreira, M. B. P. Soares and A. C. L. Leite, *Eur. J. Med. Chem.*, 2019, **180**, 191–203.
25 A. S. dos Santos Aliança, A. R. Oliveira, A. P. S. Feitosa, K. R. C. Ribeiro, M. C. A. B. de Castro, A. C. L. Leite and F. A. Brayner, *Eur. J. Pharm. Sci.*, 2017, **105**, 1–10.
26 C. M. Queiroz, G. B. de Oliveira Filho, J. W. P. Espíndola, A. V. do Nascimento, A. S. dos Santos Aliança, V. M. B. de Lorena, A. P. S. Feitosa, P. R. da Silva, L. C. Alves, A. C. L. Leite and F. A. Brayner, *Med. Chem. Res.*, 2020, **29**, 2050–2206.
27 M. Haroon, T. Akhtar, A. C. d. S. Santos, V. R. A. Pereira, L. F. G. R. Ferreira, M. Z. Hernandes, R. E. O. Rocha, R. S. Ferreira, P. A. T. d. M. Gomes, F. A. de Sousa, M. C. H. d. B. Dias, M. N. Tahir, S. Hameed and A. C. L. Leite, *ChemistrySelect*, 2019, **4**, 13163–13172.
28 C. da Silva, T. A. R. Dos Santos, I. V. B. da Silva, M. V. G. de Oliveira, D. R. M. Moreira, A. C. L. Leite and V. R. A. Pereira, *Exp. Parasitol.*, 2017, **177**, 57–65.
29 E. Izumi, T. V. J. V. F. Ueda-Nakamura, A. C. Pinto and C. V. Nakamura, *J. Med. Chem.*, 2012, **55**, 2994–3001.
30 L. P. Borba-Santos, T. Gagini, K. Ishida, W. de Souza and S. Rozental, *J. Med. Microbiol.*, 2015, **64**(4), 415–422.
31 S. Pietkiewicz, J. H. Schmidt and I. N. Lavrik, *J. Immunol. Methods*, 2015, **423**, 99–103.
32 G. F. Pauli, S.-N. Chen, C. Simmler, D. C. Lankin, T. Gödecke, B. U. Jaki, J. B. Friesen, J. B. McAlpine and J. G. Napolitano, *J. Med. Chem.*, 2014, **57**, 9220–9231.